NAVAL POSTGRADUATE SCHOOL
Monterey, California

THESIS

SIMULATION AND PERFORMANCE ANALYSIS OF THE ZONE ROUTING PROTOCOL FOR TACTICAL MOBILE AD HOC NETWORKS

by

Kevin M. Shea

September 2000

Thesis Advisor: Murali Tummala
Second Reader: Robert Ives

Approved for public release; distribution is unlimited.

REPORT DOCUMENTATION PAGE

Form Approved
OMB No. 0704-0188

1. AGENCY USE ONLY *(Leave blank)*	2. REPORT DATE	3. REPORT TYPE AND DATES COVERED
	September 2000	Master's Thesis

4. TITLE AND SUBTITLE :
Simulation and Performance Analysis of the Zone Routing Protocol for Tactical Mobile Ad Hoc Networks

5. FUNDING NUMBERS
N6600100WR00356

6. AUTHOR(S)
Shea, Kevin M.

7. PERFORMING ORGANIZATION NAME(S) AND ADDRESS(ES)
Naval Postgraduate School
Monterey, CA 93943-5000

8. PERFORMING ORGANIZATION REPORT NUMBER

9. SPONSORING / MONITORING AGENCY NAME(S) AND ADDRESS(ES)
SPAWARSYSCEN, D841 (Attn: Dr. North)
53560 Hull Street, San Diego, CA 92152 - 5001

10. SPONSORING /MONITORING AGENCY REPORT NUMBER

11. SUPPLEMENTARY NOTES
The views expressed in this thesis are those of the author and do not reflect the official policy or position of the Department of Defense or the U.S. Government.

12a. DISTRIBUTION / AVAILABILITY STATEMENT
Approved for public release; distribution is unlimited.

12b. DISTRIBUTION CODE

13. ABSTRACT ***(maximum 200 words)***

This thesis presents a simulation and analysis of the Zone Routing Protocol (ZRP) for mobile ad hoc network (MANET) environments using the OPNET simulation tool. ZRP is being suggested for possible implementation in the Joint Tactical Radio System (JTRS) for the United States military. Utilizing a ZRP OPNET model that was developed at Cornell University, the analysis focuses on key performance parameters that include overhead generation, network adaptation, efficiency, and routing zone optimization. The ZRP model's traffic monitoring has been enhanced for this work to identify the engineering tradeoffs between efficiency and performance. The results of this thesis provide valuable insight into the analysis and performance with varying zone routing radius, node velocity, and node density. Critical MANET environmental and simulation parameters required for JTRS implementation into the military battlespace have been studied.

14. SUBJECT TERMS
Joint Tactical Radio System, Mobile Ad Hoc Network, Optimum Network Performance, Protocol Analysis, Zone Routing Protocol

15. NUMBER OF PAGES
72

16. PRICE CODE

17. SECURITY CLASSIFICATION OF REPORT	18. SECURITY CLASSIFICATION OF THIS PAGE	19. SECURITY CLASSIFICATION OF ABSTRACT	20. LIMITATION OF ABSTRACT
Unclassified	Unclassified	Unclassified	UL

NSN 7540-01-280-5500

Standard Form 298 (Rev. 2-89)
Prescribed by ANSI Std. 239-18

THIS PAGE INTENTIONALLY LEFT BLANK

Approved for public release; distribution is unlimited.

SIMULATION AND PERFORMANCE ANALYSIS OF THE ZONE ROUTING PROTOCOL FOR TACTICAL MOBILE AD HOC NETWORKS

Kevin M. Shea
Major, United States Marine Corps
B.S., United States Air Force Academy, 1989

Submitted in partial fulfillment of the
requirements for the degree of

MASTER OF SCIENCE IN ELECTRICAL ENGINEERING

from the

NAVAL POSTGRADUATE SCHOOL
September 2000

Author: _____
Kevin M. Shea

Approved by: _____
Murali Tummala, Thesis Advisor

_____
Robert Ives, Second Reader

_____
Jeffrey B. Knorr, Chairman
Department of Electrical Engineering and Computer Engineering

THIS PAGE INTENTIONALLY LEFT BLANK

ABSTRACT

This thesis presents a simulation and analysis of the Zone Routing Protocol (ZRP) for mobile ad hoc network (MANET) environments using the OPNET simulation tool. ZRP is being suggested for possible implementation in the Joint Tactical Radio System (JTRS) for the United States military. Utilizing a ZRP OPNET model that was developed at Cornell University, the analysis focuses on key performance parameters that include overhead generation, network adaptation, efficiency, and routing zone optimization. The ZRP model's traffic monitoring has been enhanced for this work to identify the engineering tradeoffs between efficiency and performance. The results of this thesis provide valuable insight into the analysis and performance with varying zone routing radius, node velocity, and node density. Critical MANET environmental and simulation parameters required for JTRS implementation into the military battlespace have been studied.

THIS PAGE INTENTIONALLY LEFT BLANK

TABLE OF CONTENTS

THIS PAGE INTENTIONALLY LEFT BLANK

LIST OF FIGURES

THIS PAGE INTENTIONALLY LEFT BLANK

LIST OF ABBREVIATIONS

ABR	Associativity Based Routing
AODV	Ad Hoc On-Demand Distance Vector Routing
BRP	Border Routing Protocol
CBRP	Cluster Based Routing Protocol
CGSR	Clusterhead Gateway Switch Routing Protocol
COTS	commercial-off-the-shelf
DAG	Directed Acyclic Graph
DMR	Digital Modular Radio
DNS	Domain Name Server
DSDV	Dynamic Destination-Sequenced
DSR	Dynamic Source Routing Protocol
FSR	Fisheye State Routing
GSR	Global State Routing
HSR	Hierarchical State Routing
ICMP	Internet Control Message Protocol
IERP	Interzone Routing Protocol
IARP	Intrazone Routing Protocol
IETF	Internet Engineering Task Force
JTRS	Joint Tactical Radio System
MAC	Medium Access Control
MANET	Mobile Ad Hoc Network
NDM	Neighbor Discovery/Maintenance Protocol
OPNET	Optimum Network Performance
QD1	Quality Detection 1
QD2	Quality Detection 2
QDR	Quadrennial Defense Review
QoS	Quality Of Service
RIP	Router Internet Protocol
RFC	Request For Comments
SDR	Software Defined Radio
SSR	Signal Stability Routing
TORA	Temporally Ordered Routing Algorithm

WRP	Wireless Routing Protocol
ZHLS	Zone-Based Hierarchical Link State Protocol
ZRP	Zone Routing Protocol

EXECUTIVE SUMMARY

The Joint Tactical Radio System (JTRS) Acquisition Program was born out of the the 1997 Quadrennial Defense Review (QDR), which called for the services to combine and integrate all tactical radio equipment. The essential premise behind this project is to leverage commercial off-the-shelf (COTS) and software defined radio (SDR) technology to produce a new family of tactical radios that are multi-functional and complete with advanced data networking capabilities to meet the needs of modern information warfare. The main objective of JTRS is to interconnect radios in a mobile ad hoc network (MANET). However, conventional routing protocols are unable to meet the unique requirements of MANET. Dynamic topology, bandwidth, power limitations, and limited physical security combine to make the MANET very challenging. The first generation of JTRS, the Digital Modular Radio, is being installed in the new Marine amphibious ships currently under construction.

The Zone Routing Protocol (ZRP), developed at Cornell University, has been suggested for implementation in JTRS. ZRP incorporates a hybrid protocol which utilizes current Internet routing techniques combined with on-demand routing to reduce overhead and improve efficiency in MANET. ZRP forms a conventional Internet routing zone around each mobile node and only executes an on-demand routing protocol to meet out-of-zone destination requests. The routing zones of each mobile node provide the out-of-zone routing protocol a more efficient method of creating and establishing routes among mobile nodes.

Utilizing an OPNET model of ZRP provided by Cornell University, this thesis studied and examined the protocol's performance by developing a simple Marine tactical scenario. The focus of the analysis was on protocol overhead, network adaptation, efficiency, and optimization. Techniques and recommendations for future study of ZRP and other MANET protocols being considered for use in JTRS and DMR. The results provide a snapshot into the performance of ZRP in a simple network chosen to represent the relative scale of a single Marine rifle platoon operating in a one square kilometer area of operation.

The overhead traffic generated by ZRP was consistent with that of a hybrid MANET protocol. By adjusting the size of the conventional Internet routing zone around each node, ZRP could be optimized for the Marine scenario. The amount of overhead generated by each mobile node's routing zone was dictated by the size of its routing zone and was not impacted by mobile node velocity. The amount of overhead generated by the on-demand protocol for out-of-zone requests was dictated by the volume of traffic from each mobile node and the velocity of the mobile nodes in the network. Link performance was increased as the size of the routing zone was increased. However, the efficiency of the routing algorithm was decreased on a similar scale. The velocity of the mobile nodes had a detrimental effect on link stability. Previous techniques of optimization developed at Cornell University were also demonstrated along with the Marine scenario results.

The ZRP model utilized in this work did not incorporate several important MANET environmental factors to adequately model the JTRS battlespace. The power levels, source traffic, and antenna characteristics of each node need to be made ad hoc in nature. Furthermore, node movement should be reconfigured to provide formation movements to simulate tactical formations with appropriate movement and radio capabilities. Vehicle, foot, helicopter, and aircraft traffic could be represented by varying the velocity of some nodes. Foot mobile traffic could carry squad radios with limited transmit ranges and vehicles, helicopters, and aircraft could have greater transmitter coverage. One hundred or more MANET nodes are needed to accurately model the protocol behavior of ZRP. However, the Windows NT platform utilized for this work limited the numbers of nodes that could be placed in a scenario due to processing power limitations.

ACKNOWLEDGMENT

This thesis is dedicated to my loving wife, Amilee, who has supported me throughout this endeavor despite many hardships. I could not have done this without her constant love and support. I would also like to thank our children, Brenna and Michael, for their love and patience.

A special hand goes out to Marc Pearlman from Cornell University. I followed in the footsteps of this giant and this thesis would not have been possible had it not been for his ZRP model and continuous support and guidance along this journey.

I would like to thank my thesis advisor, Dr. Murali Tummala, for his research guidance, direction, and mentorship. My fellow research colleagues, Dr. Robert Ives (LCDR USN), Capt Ty Theriot (USMC), and Lt Leonardo Mattos (Brazilian Navy), were sources of encouragement and support.

Finally, I would like to thank the Marine Corps for giving this Marine a chance to pursue an advanced degree in electrical engineering. This opportunity could not have been realized without the confidence and support of the men and women in uniform whom I've had the pleasure of serving across the globe in both peace and war.

THIS PAGE INTENTIONALLY LEFT BLANK

I. INTRODUCTION

The Joint Tactical Radio System (JTRS) Acquisition program was born out of the 1997 Quadrennial Defense Review (QDR), which called for the services to combine and integrate all tactical radio development [1]. The essential premise behind this project is to leverage commercial-off-the-shelf (COTS) and software defined radio (SDR) technology to produce a new family of tactical radios that are multi-functional and complete with advanced wireless data networking capabilities to meet the needs of modern information warfare. The most aggressive objective of JTRS is the ability to form the radios into a mobile ad hoc network (MANET) [1]. The first generation of JTRS, the Digital Modular Radio (DMR), has been incorporated into Marine amphibious shipping currently under construction (LPD-17).

Conventional routing protocols are unable to meet the unique requirements of MANET. Dynamic topology, bandwidth and power limitations, and limited physical security combine to make the MANET environment challenging [2]. All facets of MANET exhibit ad hoc behavior; bit rates, quality of service (QoS), infrastructure, mobility patterns, and mobility characteristics [3]. This wide range of operating configurations poses an enormous challenge to routing efficiency. Traditional shortest-path routing algorithms, such as the Distributed Bellman-Ford (DBF) algorithm, incur large update message penalties and exhibit slow convergence [3]. The requirement to reduce overhead and improve convergence has driven researchers to examine protocols with proactive path finding algorithms, which combine distance vector and link state approaches [3]. On-demand discovery of routes can result in further overhead reductions compared to table-driven methods (e.g. link-state and distance vector), but suffer from latency due to route discovery delays. A hybrid combination of on-demand and proactive techniques has produced a more efficient routing protocol [2].

The Zone Routing Protocol (ZRP), developed by Haas and Pearlman [4], incorporates a hybrid protocol that exploits the benefits of both reactive and proactive protocols and has been suggested for possible implementation in the Joint Tactical Radio System (JTRS) for the United States military [1]. In ZRP, each node has a proactive zone around it, which is dictated by an adjustable zone routing radius. The zone routing radius is directly related to hop counts from the node. Routes outside the zone are determined by a reactive query that leverages the zone structure of the MANET using ZRP. The intent behind this MANET routing approach is to leverage routing knowledge in a

localized region and reach out to selected network nodes as opposed to flooding a network to locate a destination.

The objective of this thesis is to study and analyze the Zone Routing Protocol (ZRP) for MANET environments using an OPNET simulation provided by Haas and Pearlman [4]. The focus of the analysis will be on protocol overhead, network adaptation, efficiency, and routing zone optimization. Furthermore, the objective is to produce techniques and recommendations for future application of ZRP and other MANET protocols being considered for use in the JTRS and DMR. The results presented provide a snapshot into the performance of ZRP in a small generic network chosen to represent the relative scale of a single Marine rifle platoon operating in a one square kilometer area of operation.

Chapter II begins with an introduction into the MANET environment and routing protocols. Hierarchical State Routing (HSR) and Temporally Ordered Routing Algorithm (TORA) are used to illustrate MANET protocols. The third chapter introduces ZRP and explains its method of operation. Chapter IV provides the reader with an understanding of the ZRP model and OPNET package used in this work. Chapter V presents the results of the simulation and analysis. Conclusions and recommendations are included in the final chapter.

II. MOBILE AD HOC NETWORK PROTOCOLS

A MANET is a network environment where both the user nodes and the infrastructure itself are constantly in transition. There is no reliance on pre-existing fixed infrastructure, such as wireline backbone or network connectivity via satellite links. MANETs are intended to function independent of the fixed infrastructure with the exception of a few "stub" gateways to provide access to the larger network. Figure 1 provides an illustration of the differences between MANET, traditional fixed

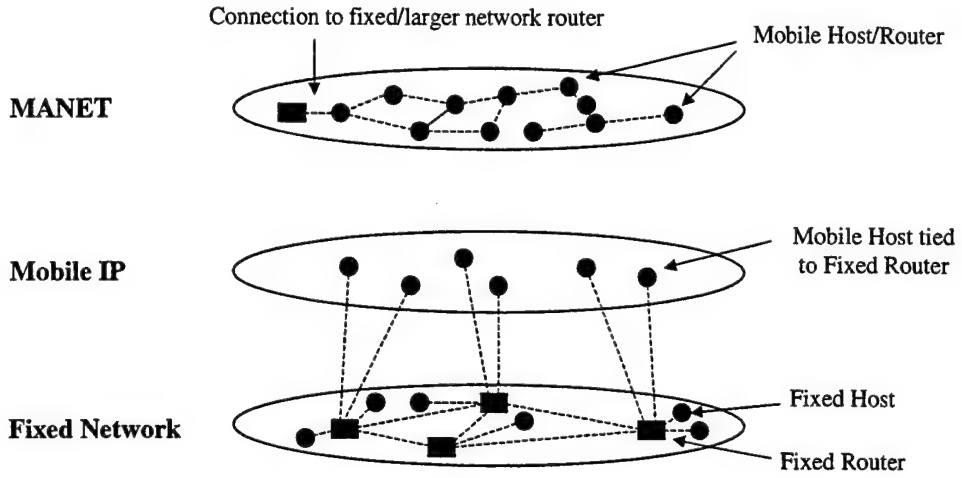

Figure 1. MANET Layer In Perspective (After Ref. [2]).

Internet, and Mobile IP. The traditional fixed Internet is stable with little or no host/router mobility. Mobile IP attempts to give the hosts more mobility, but still requires a connection to the fixed network. As depicted in Figure 1, a MANET node is truly mobile and is itself a router with multiple wireless or wired connections. A MANET has four distinct characteristics, which together form unique underlying assumptions, design considerations, and concerns that are not revealed in static networking: dynamic topology, bandwidth constraints, energy constraints, and limited physical security [2]. Communication protocols for this demanding environment must be adaptable, self-organizing, robust, and efficient enough to meet the constrained resources. Conventional routing protocols associated with a static, fixed infrastructure internet are unable to meet the unique requirements in a MANET environment due to considerable overhead and slow reaction to topological changes.

In a MANET, each node has a unique internet protocol (IP) address. Routers use a routing protocol to learn about the network and to determine the optimal path for sending a packet to a destination. The routing protocol functions at the network layer (see Figure 2) to perform this function. MANET protocols utilize the following basic services from the lower three levels: link status, packet delivery, and network layer address [2]. The following sections will examine conventional and MANET routing protocols in more detail before looking at ZRP in Chapter III.

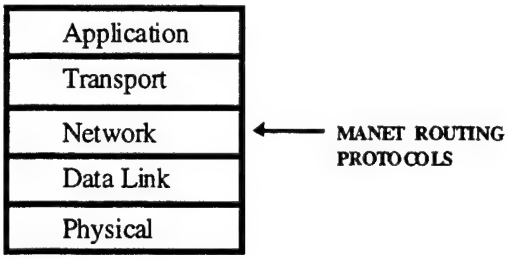

Figure 2. Typical Protocol Stack for MANETs.

A. CONVENTIONAL ROUTING PROTOCOLS

Conventional routing protocols use either distance vector or link-state algorithms to determine the most efficient path to a destination. Distance vector algorithms require each router to maintain a table with routes to all possible destinations along with an associated metric that is collected on a periodic basis. The routing overhead remains constant regardless of the amount of host movement. This type of method is closely associated with the distributed Bellman-Ford routing alogrithm. A version of Bellman-Ford is still being used today with the Router Internet Protocol (RIP). In RIP, for each entry the next hop to the destination is stored along with a metric to reach the destination. The metric can be based on distance, total delay, or the cost of sending the message [5]. Each node shares its internal information periodically through update broadcasts to neighboring nodes. The routers utilize the updates to constantly revise their routing tables for shortest-path calculations. Link-state algorithms operate in a similar manner but are event driven by changes in the link status of nodes. Path-finding algorithms provide a hybrid approach utilizing both distance vector and link-state algorithms [13].

Although distance vector and link-state algorithms are very effective for achieving routing optimization, the overhead associated with these techniques is considerable and exhibits slow convergence due to topological changes. A simulation study was conducted

by Lee, Gerla, and Toh [5], which analyzed RIP in a MANET and highlighted shortfalls of conventional routing protocols. In RIP, a conventional protocol, routing updates are produced on a periodic basis. According to the study, RIP does not scale well to large networks, because each network node requires N iterations to detect a node that is disconnected, where N represents the number of nodes. This is known as the *count to infinity* problem. On-demand protocols have clear proportional increase in overhead due to node mobility. Figure 3 depicts the overhead associated with periodic, on-demand, and hybrid protocols as a function of mobility. As clearly shown in Figure 3, the study determined that a hybrid proctocol is needed to meet the requirements of MANET.

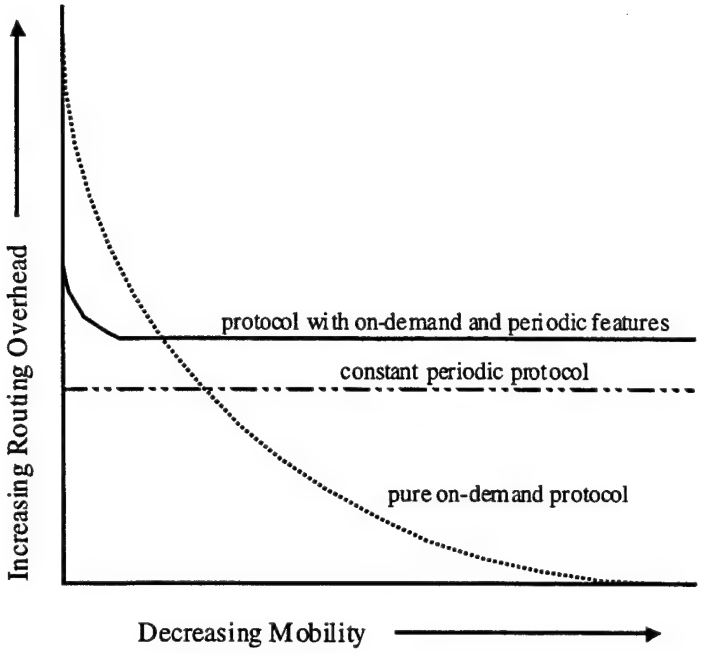

Figure 3. Behavior of On-demand and Periodic Mechanisms (From Ref. [6]).

B. TABLE DRIVEN VS ON-DEMAND PROTOCOLS

Two distinct types have emerged from the development of MANET protocols: table-driven and on-demand [7]. In table-driven algorithms, current routing information is maintained at each node. Table-driven algorithms are adaptations of the distance vector and link-state techniques. The constant routing updates, different types of tables, distributions, and techniques are used to increase efficiency. In contrast, on-demand protocols attempt to reduce overhead and are more responsive to MANET by having the source node dictate requirements. Routes are created on an as-required basis by the

source node. As depicted in Figure 3, a hybrid protocol combining both periodic and on-demand qualities responds to the needs of the network without creating excessive traffic overhead. All routes created, both on-demand and periodic, hold a time stamp to eliminate outdated routes.

There are several types of MANET protocols being considered by the Internet Engineering Task Force (IETF) MANET Working Group that are table-driven (periodic) or on-demand. Some examples of table-driven MANET protocols are the Dynamic Destination-Sequenced (DSDV), Wireless Routing Protocol (WRP), Global State Routing (GSR), Fisheye State Routing (FSR), Hierarchical State Routing (HSR), Zone-based Hierarchical Link State Protocol (ZHLS), and Cluster Head Gateway Switch Routing Protocol (CGSR). DSDV is based on the classic Bellman-Ford algorithm. WRP is a table-based distance vector routing protocol. GSR is similar to DSDV, but takes the idea of link-state routing and improves it by limiting the flooding of table updates. FSR improves on GSR by limiting the size of update broadcasts. ZHLS is similar to HSR and divides the network into non-overlapping zones, but unlike HSR, there is no cluster head. CGSR is a combination of ZHLS and DSDV. Examples of on-demand MANET protocols include the Cluster Based Routing Protocol (CBRP), Ad Hoc On-Demand Distance Vector Routing (AODV), Dynamic Source Routing Protocol (DSR), Temporally Ordered Routing Algorithm (TORA), Associativity Based Routing (ABR), and Signal Stability Routing (SSR). GBRP combines the cluster technique with on-demand routing. AODV is a combination of DSDV and on-demand routing. DSR is an on-demand protocol initiated by the source node and focuses on route discovery and route maintenance. ABR defines a new routing approach with a metric based on link stability. SSR also defines a new metric approach based on node signal strength and location stability. HSR and TORA will be explained in the following sections to introduce a protocol from each category.

1. Hierarchical State Routing (HSR)

HSR combines the ideas of zone routing with a hierarchical structure and is clearly linked with conventional table-driven protocols. As depicted in Figure 4, nodes are broken up into routing zones at the physical network layer and selected nodes (cluster heads) become members of a virtual hierarchical tree similar to that in the Internet. Routing information is controlled in a tree data structure fashion. Each routing zone on the physical layer is tied together by a cluster head, which serves as the virtual leader of

the routing zone. The cluster head is periodically elected and collects all the routing data from the zone and distributes all the zone's routes to other cluster heads on a virtual layer. The cluster heads provide the medium to share routing information in a hierarchical tree architecture. Selected cluster heads are promoted to higher levels in the tree data structure up to the root node and pass routing information among themselves on virtual layers. The cluster heads serve as the conduit to the upper and lower level cluster heads to ensure that all routing information is distributed to all levels. A gateway node is a node that resides in more than one zone and can communicate with nodes in both zones.

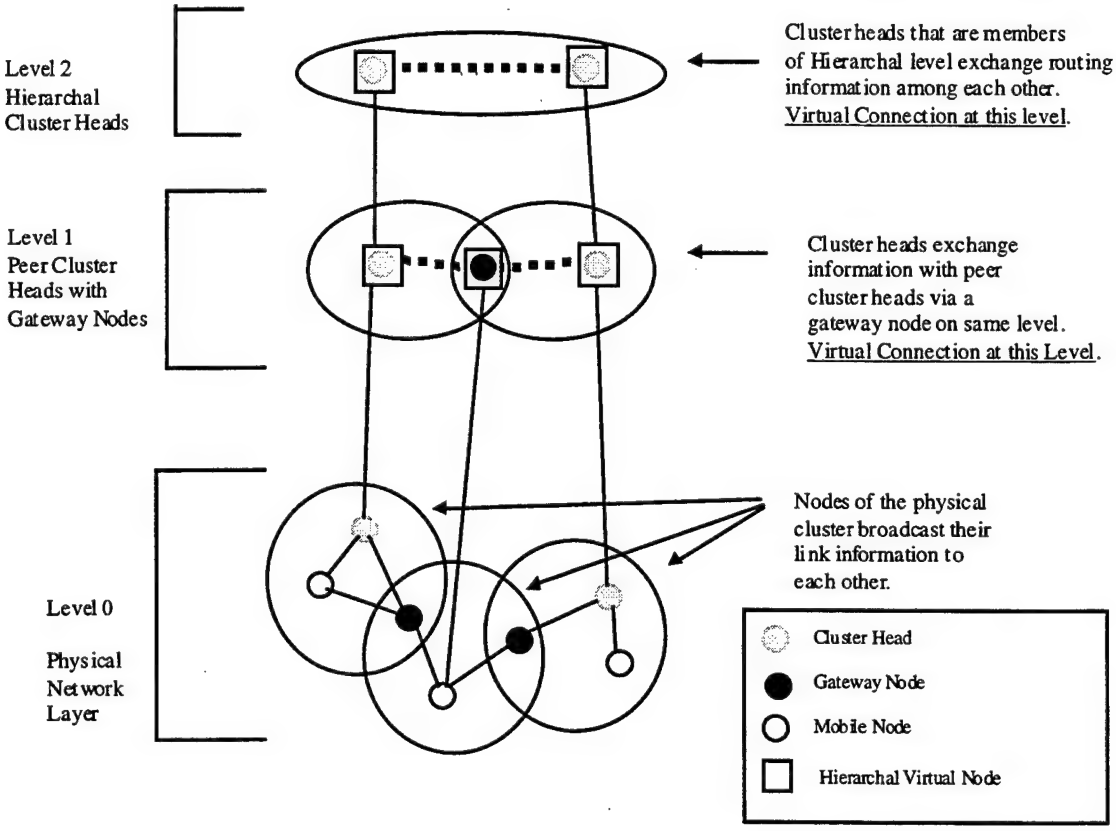

Figure 4. An Example of Clustering in HSR (After Ref. [7]).

As shown in Figure 4, the nodes are partitioned into subnetworks (Level 0, Level 1, and Level 2) according to the respective level in the hierarchical tree structure. A Location Management Server (LMS) handles address assignments for each subnetwork. Nodes that desire to operate in the subnetwork must register with the LMS to obtain an address. Each node is assigned a logical address <subnet,host> by their respective LMS.

The LMS functionality is similar to that of a Domain Name Server (DNS) in the Internet and shares information with other LMS to distribute routing information.

2. Temporally Ordered Routing Algorithm (TORA)

The Temporally-Ordered Routing Algorithm (TORA) was developed by Park and Corson and is presented in detail in a 1997 draft RFC [8]. It is a source-initiated, on-demand routing protocol proposed for dynamic mobile, multihop wireless networks. TORA is an adaptive, efficient, and scaleable distributed routing algorithm based on the concept of link reversal. The main feature of this protocol is the ability to localize control messages in a very small set of nodes which must respond to a change in network status, such as a link failure. This is accomplished by each node maintaining an extensive routing cache. The cache memory leads to scalability problems in large networks when memory requirements become excessive. The protocol is designed to work on top of the MAC layer that handles link status, packet delivery, link and network layer address resolution, and security authentication [8].

In TORA, the source node initiates the route creation since it is an on-demand routing protocol. The algorithm looks to build a directed acyclic graph (DAG) representing the relative heights of the routers with reference to the destination. Routers that are closer to the destination have a low height and are referred to as downstream nodes. Routers that are farther away from the destination typically have ever-increasing heights and are referred to as upstream nodes. Figure 5 presents an illustration of a directed acyclic graph formed when creating routes by relative heights of routers [9]. The height metric is maintained by an ordered quintuple (τ, oid, r, δ, i) , where τ is the logical time of a link failure defining a new reference level, oid is the unique ID of the router that defined the new reference level, r is a reflection indicator bit, δ is a propagation ordering parameter, and i is the unique ID of the router [8].

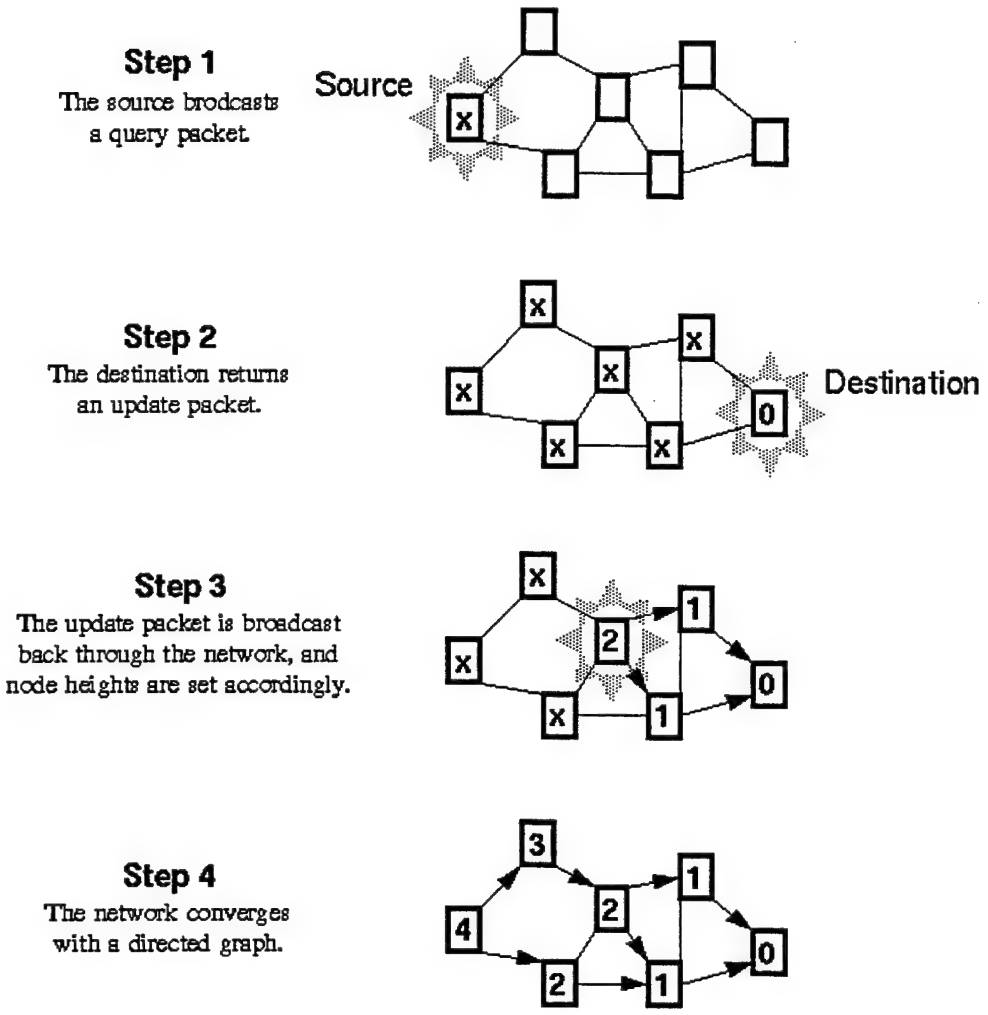

Figure 5. TORA Route Creation (From Ref. [9]).

C. EVALUATION OF MANET PROTOCOLS

There is no standard for evaluating MANET protocols. The IETF MANET Working Group recommends focusing on the fundamental tenets of MANET [2]. MANETs exhibit ad hoc behavior across the board. Bit rates, time constraints, reliability requirements/QoS, infrastructure, mobility patterns, and mobility characteristics (speed, predictability, and uniform) are all ad hoc in nature [3]. Evaluation is even more challenging when one considers that mobile wireless assets will have limited range, packet loss, mobility loss, limited power, frequent network partitions, and security vulnerability.

The MANET Working Group emphasizes that each MANET Routing Protocol is well suited for particular MANET environments, and less suited for others. Each protocol should be evaluated in terms of advantages and disadvantages as opposed to one common test for all protocols [2]. The Working Group identifies eight networking environment variables for examination: network size, network connectivity, topological rate of change, link capacity, fraction of unidirectional links, traffic patterns, mobility, and fraction and frequency of sleeping modes. Placing emphasis on intricate protocol comparisons is of limited value [7]. The results are often imprecise and make it difficult to compare algorithms with vastly different functionality in a precise, fair, and meaningful fashion. What is important is the average performance, which is only obtained through simulation.

Metrics utilized for evaluation should be independent of the network protocol and both qualitative and quantitative. The Working Group identifies the following qualitative metrics: distributed operation, loop freedom, demand-based operation, proactive operation, security, sleep period operation, and unidirectional link support. Quantitative metrics identified are the following: end-to-end data throughput, delay, route acquisition time, percentage of out-of-order delivery, efficiency, average number of data bits transmitted divided by data bits delivered, average number of control bits transmitted/data bit, and average number of control and data packets transmitted divided by data packets delivered.

The most important factor affecting performance is how well the propagation of redundant copies of a route discovery request by a mobile can be reduced to conserve memory cache [10]. An algorithm should recognize and discard identical requests and if a request has identified a route beyond a maximum length. The maximum length restriction serves to prevent infinite loops from occurring during discovery. However, aggressive route cache to enhance routing tables and the use of cache are critical parameters which prevent latency and unnecessary queries.

III. ZONE ROUTING PROTOCOL (ZRP)

The ZRP protocol, developed by Haas and Pearlman [11], incorporates a localized zone approach to routing. The fundamental approach is to incorporate a hybrid protocol that exploits the benefits of both a reactive and a proactive protocol [12]. As depicted in Figure 6, each mobile node has a proactive routing zone around it that is dictated by an adjustable zone routing radius. The zone routing radius is directly related to hop counts from the node. In Figure 6, nodes D, C, F, B, and E are in Zone A with zone routing radius $\rho = 2$. Routes outside the zone are determined by an on-demand protocol query which bordercasts the out of zone query to the peripheral nodes (D, F, and E), which in turn, leverage the zone structure of the network to reduce query detection time. The intent behind this MANET routing approach is to utilize the routing knowledge in a localized region and obtain a route to a distant node on-demand. The following discussion on ZRP will focus on three major areas: Intrazone Routing Protocol (IARP), Interzone Routing Protocol (IERP), and routing optimization.

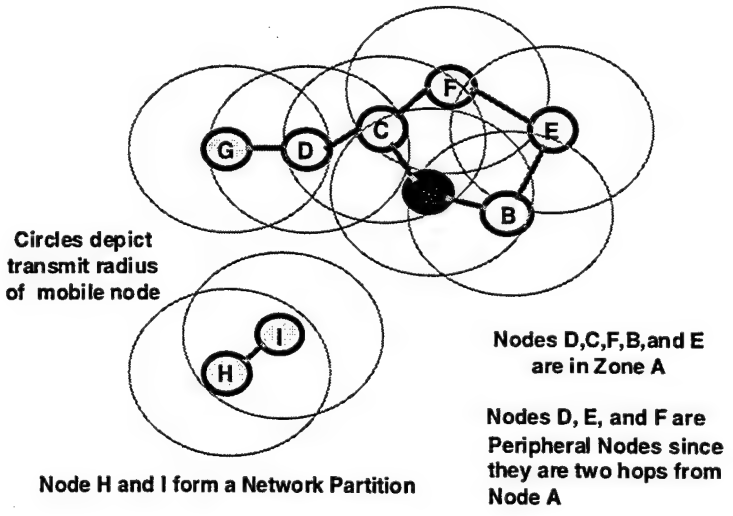

Figure 6. ZRP Example With Zone Routing Radius $\rho = 2$.

A. INTRAZONE ROUTING PROTOCOL (IARP)

IARP is responsible for maintaining routes within each node's routing zone through periodic routing table updates. This is usually accomplished using a wide range of traditional distance vector or link-state protocols [3]. All nodes less than or equal to

the routing zone radius are considered to be in the zone. These nodes are referred to as interior nodes. Nodes on the edge of the routing zone (those with hop count equal to the zone radius) are considered peripheral nodes and take on greater significance in the next section. Figure 6 depicts a typical zone centered around Node A with $\rho = 2$. The peripheral nodes reside at the outermost limit of the zone radius. In this case, D, F, and E are examples of peripheral nodes.

Regardless of the reactive protocol chosen, it needs to be modified to keep the proactive traffic generation within the region of an individual node's routing zone. For example, a split horizon version of the Distance-Vector Algorithm can be utilized for IARP. Although there are tradeoffs involved in IARP protocol selection, experience has shown that the overall performance of ZRP is not affected by this choice [4]. As shown in Figure 7, IARP relies on the Neighbor Discovery/Maintenance Protocol (NDM) to provide current status of a node's neighbors. This NDM service is provided by the MAC/link-layer protocols. Overhead is not spared in the region for the sake of proactive discovery. Routing within each region should be fairly routine and not require much discovery effort outside of the proactive efforts. The overhead generated with this scheme is a function of the number of nodes in the routing zone (node density) and the zone routing radius [12]. Node density is a function of transmit radius.

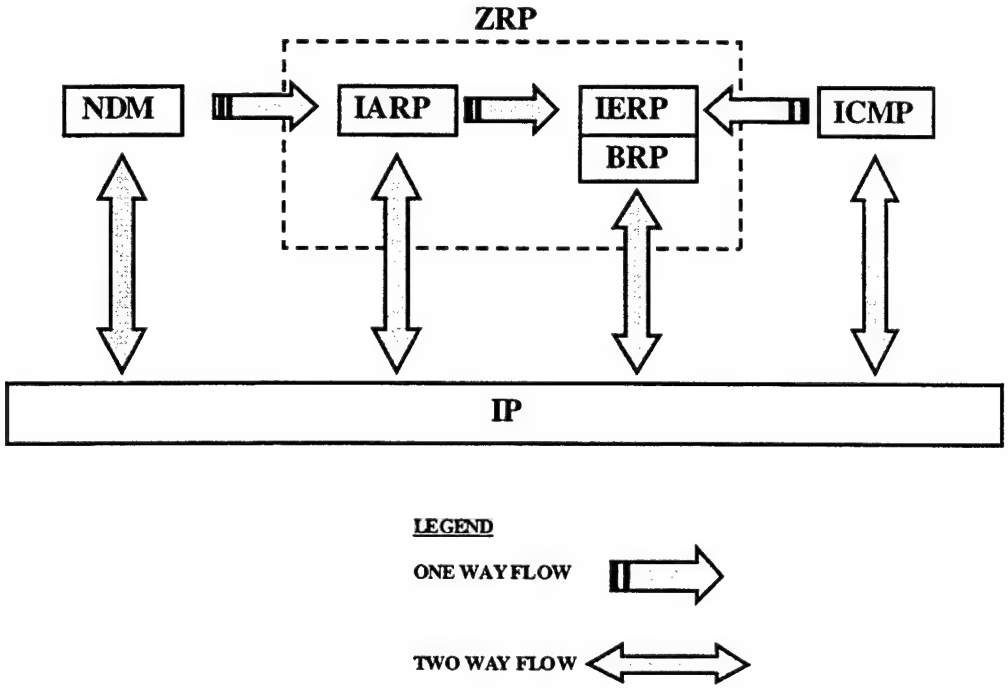

Figure 7. ZRP Architecture (After Ref. [11]).

It is important to remember that the wireless nature of MANET can cause high zone populations despite a small hop count. As mentioned above, the physical coverage of the transmit antenna and the receiver density (per unit area) dictate the number of nodes in the zone (node density). The result is a significant increase in proactive IARP traffic and increased contention within the local zone [4]. Each MANET environment is characterized by the number of nodes N, node density δ, and relative node velocity ν. The routing zone radius ρ ranges from the reactive region ($\rho = 0$) to the proactive region ($\rho \rightarrow \infty$). The amount of IARP traffic per node (T_{IARP}) can be expressed by

$$T_{IARP} = \nu \times U_{IARP} / N_{neighbor}$$

where U_{IARP} is the number of IARP updates and $N_{neighbor}$ is the number of neighbors per node [4]. The amount of IARP traffic per node does not depend on the total node population, but it is a function of the the size of ρ. $N_{neighbor}$ is a function of both ρ and δ [14].

B. INTERZONE ROUTING PROTOCOL (IERP)

Routing outside the zone is done based on a reactive or on-demand approach, by using IERP. Some of the functions of IERP including bordercasting, route accumulation, and query control, are performed by a special component of IERP called the Bordercast Resolution Protocol (BRP) (see Figure 7). IERP queries through the network, although global in nature, are expedited through the use of proactive routing zones. Instead of having to reach each node, the discovery process must merely touch each routing zone to discover the targeted node. When IERP queries are compared to a flooding mechanism, efficiency is increased and overhead is decreased by utilizing the zone topology of the network. The number of nodes queried (N_q) in the MANET is on the order of ($\mathcal{O}$)

$$N_q \approx \mathcal{O} (\rho_{zone} / \rho_{net})^2$$

where ρ_{zone} is the zone routing radius and ρ_{net} is the network radius [13].

The amount of route usage will vary due to applications and is expressed by two independent parameters: $R_{initial\text{-}query}$ and $R_{route\text{-}usage}$ [4]. Route stability is dictated by route lengths and is a factor of the span of the network, node velocity ν, node density δ, and

zone radius ρ. Stability is expressed in terms of lifetime and is represented by its inverse, the average route failure ($R_{route\text{-}failure}$). The amount of IERP traffic (T_{IERP}) is represented by

$$T_{IERP} = T_{qN}(\rho, \delta) \times T_{query}$$
$$= T_{qN}(\rho, \delta) \times N \times (R_{initial\text{-}query} + R_{subsequent\text{-}queries})$$

where T_{query} is the rate of traffic queries, N is the number of network nodes, and T_{qN} is traffic per queries per node and is a function of ρ and δ [4].

Routing failures are detected and repaired reactively by IERP. However, route failures can be detected by IP when a source route is determined to be unreachable. As shown in Figure 7, a route failure notification is usually provided by protocols, such as the Internet Control Message Protocol (ICMP). The repair process initiated by IERP is almost identical to the discovery process. IARP utilizes proactive route failure detection, which is triggered in response to a node leaving the source node's zone by the NDM mechanism.

1. Border Routing Protocol (BRP)

Before examining the routing process, it is important to understand the structure of the localized nodes and the concept of bordercasting. As depicted in Figure 7, BRP is a subset and the workhorse of IERP. It provides bordercasting, route accumulation, route optimization, and query control [14]. As stated earlier, each zone is centered on a node and the size is dictated by the radius which can be modified for efficient routing in various types of networks [4]. When a node must reach a destination outside of the zone, efficiency is increased by bordercasting the query request directly to the peripheral nodes to reach the entire network. BRP uses efficient flooding (multipoint relay) and efficient probing to control unnecessary overhead. It also does proactive route repair and route shortening to improve performance. This reduces the overhead in comparison to simple flooding over the entire network. IERP provides the route retrieval and route failure functions once the route is identified.

Due to the extensive proactive discovery of IARP, a node can efficiently reach another node within the zone. As mentioned above, BRP provides the route optimization inside each zone [14]. When a node must be reached outside of the zone, this process is made more efficient by now exploiting the zonal topology of the network. With a quick

table look up, the node is able to first determine if the destination is within the node's zone. Once this factor is eliminated, the query is quickly bordercasted to the peripheral nodes to initiate the broader search. The peripheral nodes' neighbors cast to their respective neighbors not in the region, and each neighbor node is able to quickly determine if the prospective destination node is within its zone. If not found in the neighbor zone, the neighbor nodes in turn will bordercast across their zones, and the process continues until the destination node is located. Once the destination node is located, IERP returns the requested route to the source node which has been optimized by BRP using the proactive routing information stored in each zone by IARP.

Figure 8 illustrates the discovery process used in IERP. Node A has a datagram to send to L. As depicted, L is not in A's routing zone. Node A bordercasts (BRP) the route query to all peripheral nodes (D, E, F, and G). Each peripheral node, in turn, checks its routing table (IARP) for L and none of them have it. Each peripheral node now bordercasts (BRP) to its own peripheral nodes. For example, Node G conducts a table look up from its zone table (IARP) and is unable to locate node L. A bordercast (BRP) is initiated by node G, and K is able to check its table (IARP) and quickly respond (IERP) with the location of node L. The return route is identical to the query route.

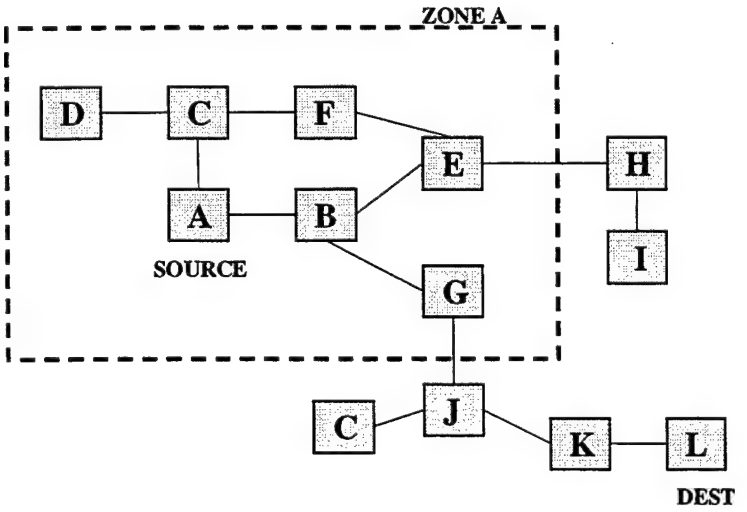

Figure 8. IERP Search with BRP (From Ref. [11]).

ZRP does incorporate a query detection mechanism to reduce redundant queries and prevent it from degenerating to a flooding protocol [4]. ZRP offers two distinct methods of query detection for redundant queries and reduce overhead. Query Detection 1 (QD1) allows the intermediate nodes to detect a redundant query and terminate the

thread. Query Detection 2 (QD2) allows all nodes to detect a redundant query and terminate the request.

C. ROUTING ZONE OPTIMIZATION

A mathematical expression for the optimum zone radius for optimum performance has not yet been determined [4]. Even with perfect knowledge of all network parameters, computation of an optimal routing zone radius is not a straightforward mechanism. Haas [4] recommends that further research could focus on a complete derivation of the ZRP traffic function. As depicted in Figure 9, a simple approach is to adjust the zone routing radius until the setting for minimum ZRP overhead traffic is achieved. In the interim, two other schemes have been suggested for optimum

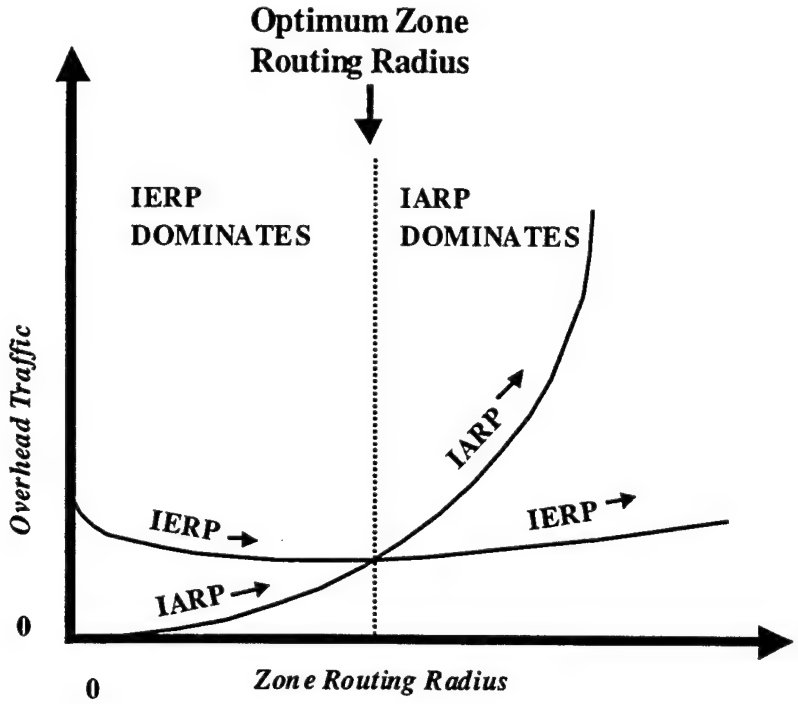

Figure 9. ZRP Zone Routing Radius Optimization.

zone routing radius selection: min-searching and traffic adaptive method [4]. Min-searching assumes that the node behavior will not change quickly over a period of time and an accurate assessment of ZRP traffic can be obtained. As shown in Figure 9, if IERP traffic is decreasing and the amount of proactive IARP traffic is increasing, there is an "undershoot" of the optimum zone radius. Likewise, if IERP traffic is increasing and

IARP traffic is also increasing would indicate an "overshoot" of the optimum zone radius. The traffic adaptive method only relies on current estimates. In this case, Haas [4] has shown that the amount of ZRP traffic generated is significantly higher when the ZRP traffic is dominated by the reactive IERP query traffic. The same is true when IARP traffic dominates. As depicted in Figure 9, the optimum region resides between these two regions. In other words, the ratio between IERP to IARP (IERP/IARP) should be as close one as possible for optimization. The general rule-of-thumb is that a sparse network favors a large routing zone and a dense network favors a small routing zone.

D. SUMMARY

Chapter III has presented the ZRP protocol and the three main component protocols: IARP, IERP, and BRP. ZRP establishes a routing zone around each node in the MANET environment. The size of each routing zone is dictated by an adjustable zone routing radius. Within each routing zone, IARP is responsible for maintaining routes through periodic routing table updates. All nodes less than or equal to the routing zone radius are considered in the zone. Routing outside the zone is done using a reactive on-demand protocol, IERP. BRP, a subset of IERP, provides bordercasting, route accumulation, and query control. IERP queries outside the zone are propagated by the use of the proactive routing zones defined in the MANET. ZRP optimization is achieved by balancing IERP and IARP overhead traffic. The optimum zone routing radius resides in the region where the ratio between IARP and IERP overhead is equal to one. The min-searching and traffic adaptive method are two alternative techniques for locating the optimum zone routing radius.

THIS PAGE INTENTIONALLY LEFT BLANK

IV. SIMULATION

The simulation software used in this thesis was OPNET, Version 7.0 on a Windows NT platform. Pearlman's ZRP OPNET implementation, developed in a UNIX environment, was the only MANET protocol available at the time of this work and was made available to the author. The UNIX based model was modified by the author through extensive collaboration with Pearlman [14] for implementation into a Windows NT environment. The OPNET package was chosen for this MANET protocol research due to its availability at the Naval Postgraduate School (NPS). Other popular simulation software packages used for MANET protocol simulation include ns2, PARSEC, and the C programming language.

A. OPTIMUM NETWORK PERFORMANCE (OPNET)

OPNET Version 7.0 can be used to simulate most standard network protocols and IEEE standards. For example, this most recent version has the ability to simulate IEEE 802.11 for wireless networks. There is an extensive model library with easy to follow instructions and examples. However, MANET protocols are not yet standard with OPNET. The models can be broken down into three distinct levels as depicted in Figure 10. The network layer depicts the *network objects* needed for network implementation. Each element (e.g., computer, bridge, router) in the *network model* is composed of a *node model*, which is further subdivided into *node objects*. For example, in Figure 10, *udp*, *rsvp*, *ip_encap*, and *application* are *node objects* of the *workstation* node model. The *node object* behavior is modeled by *process models* which actually contain the C code and OPNET specific *kernel procedures.*

The C code and kernel procedures in an OPNET simulation are only executed in three locations which all reside in the *process model states.* As depicted in Figure 10, a stop sign-like icon represents a *wait* state. There are three types of states: initial, unforced, and transitional. The initial and unforced states appear as red stop signs and the transitional state appears as a green stop sign. *Transitions* form the connections between states. Within the stop signs, there are *Enter Execs* and *Exit Execs* where code is executed. As shown in Figure 10, the *Exit Execs* of the *wait* state appear in the lower right hand window. An unforced state will execute the *Enter Execs* code and return control to the processor while awaiting for a transition condition. Simulation time only expires between unforced states and processor handoffs. If a transition is identified in the

form of a code interrupt, transition code will be executed by the green transition states or by code resident in the transition link itself. For example, in Figure 10, a *default* transition condition forces a return to the *wait* state in the event of an unpredicted condition.

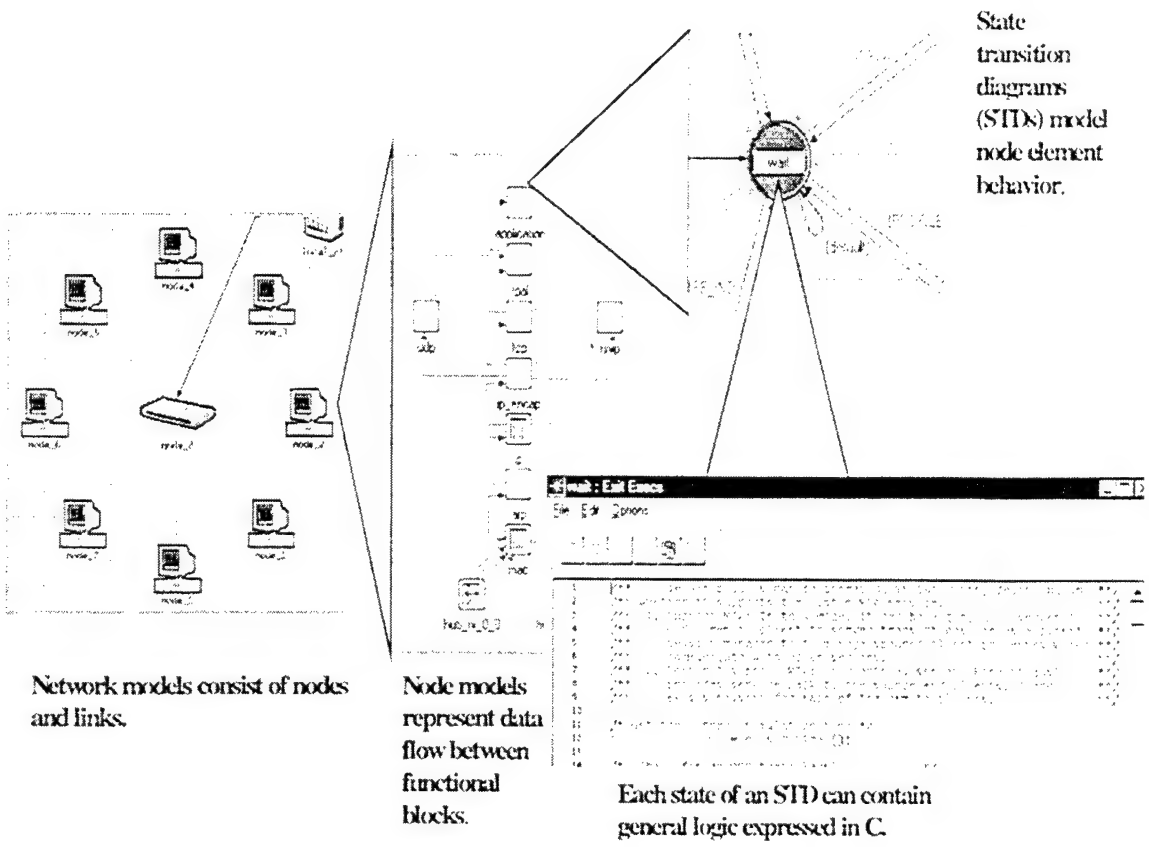

Figure 10. OPNET Simulation Methodology From Ref. [15].

B. ZRP MODEL

The ZRP OPNET model is implemented by placing individual MANET mobile ZRP network objects, called *manet_ls*, in the workspace to create a network model. Figure 11 depicts a typical network model configuration *manet_ls* of network objects positioned in a workspace. Each *manet_ls* has behavior driven by the node model. The *manet_ls* node model is depicted in Figure 12 and illustrates the *various node objects* required to implement *manet_ls*: routing *(routing),* movement *(move),* transceiver *(tx_simple* and *rx_simple*), MAC (*delivery* and *beacon*), and traffic generation (*app*). The

node objects of *manet_ls* are explained in further detail in the following sections. The number of *manet_ls* ZRP nodes in the *network model* is limited to approximately 1000 [14]. The user is able to manipulate the following variables for each simulation: zone routing radius ρ in hop count, node velocity ν in km/sec, transmit radius t_r in km, and the duration of simulation (time units as appropriate). The node movement field is two dimensional and defined by an *x_axis* and *y_axis* entry (km).

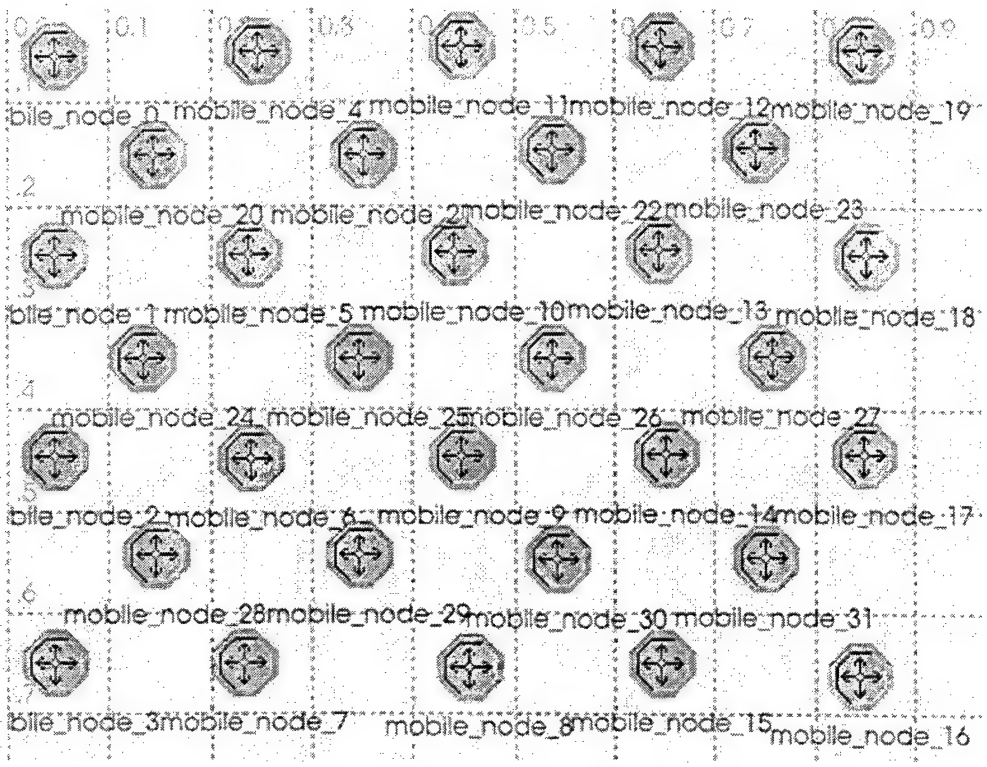

Figure 11. ZRP Network Configuration.

1. Routing and Traffic Generation

As depicted in Figure 12, the *routing* node object is the key to the ZRP model's routing performance. From *routing*, the traffic is passed to the appropriate-routing protocol for processing as explained in Chapter III. *IARP* handles the in-zone traffic. *IERP* and *BRP* handle the out-of-zone traffic. Figure 13 is provided to illustrate the node object, *routing,* within *manet_ls*. In this depiction, a query packet has arrived at *routing* after being routed to *IARP* (see Figure 14) to determine if the destination node was located in the source node's routing zone. The destination node was not located in the routing zone so the *routing* mechanism passes the query packet to *BRP* (see Figure 15) for bordercasting which interacts with *IERP* (see Figure 16) to provide route

accumulation until the destination node is located. *IERP* provides the route reply notification to the source node. As the process model executes through the *xmit* transition state, the *Enter Exec* code depicted is executed, which records the amount of overhead traffic being generated to meet the query requirement.

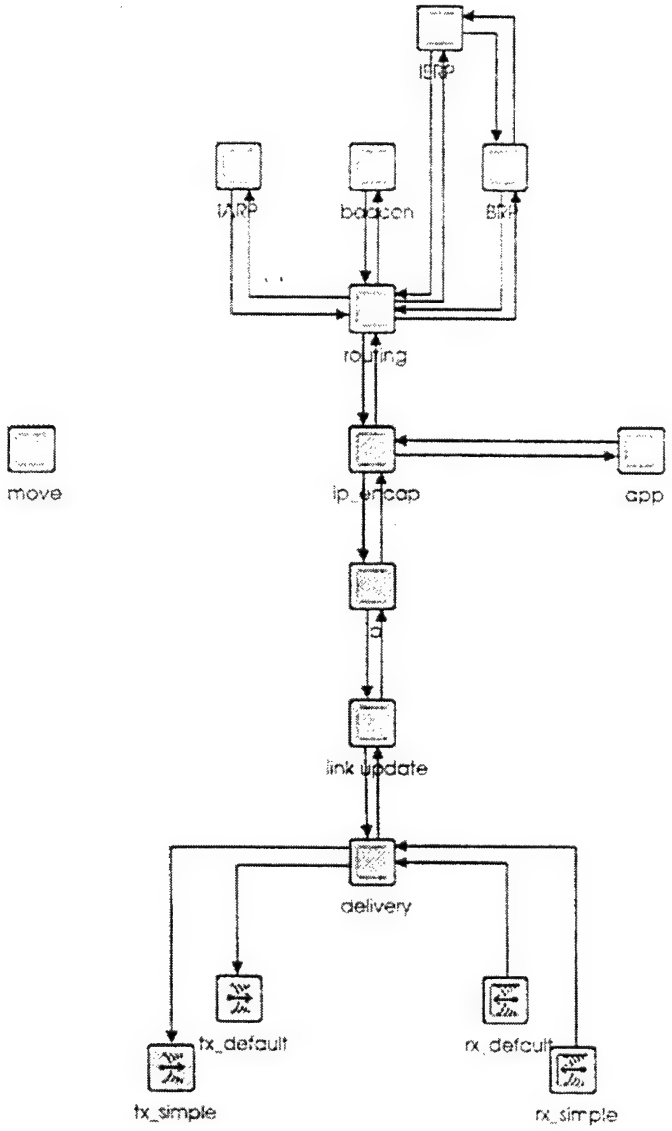

Figure 12. Manet_ls Node Model.

The *beacon* module is part of a neighbor discovery action which is typical of most MAC protocols and independent of ZRP [4]. The MAC neighbor discovery components, *beacon* and *delivery*, shown in Figure 12, were purposely included in *manet_ls* to provide an ideal MAC behavior for comparison with various MAC protocols. The MAC layer

provides ideal scheduling of packet transmissions to avoid collisions. This feature allows for delays produced by various MAC protocols to be isolated. It has been shown that the MAC protocol has little effect on the overall performance of ZRP [4]. The IARP traffic is generated based on a change in a neighbors status which is updated every $2T_{beacon}$ (0.5 seconds) for link status. The amount of IARP traffic is independent of the total network population and dictated by node density and the zone routing radius. IERP traffic is distributed on a uniform random traffic queries initiated by the *app* process model.

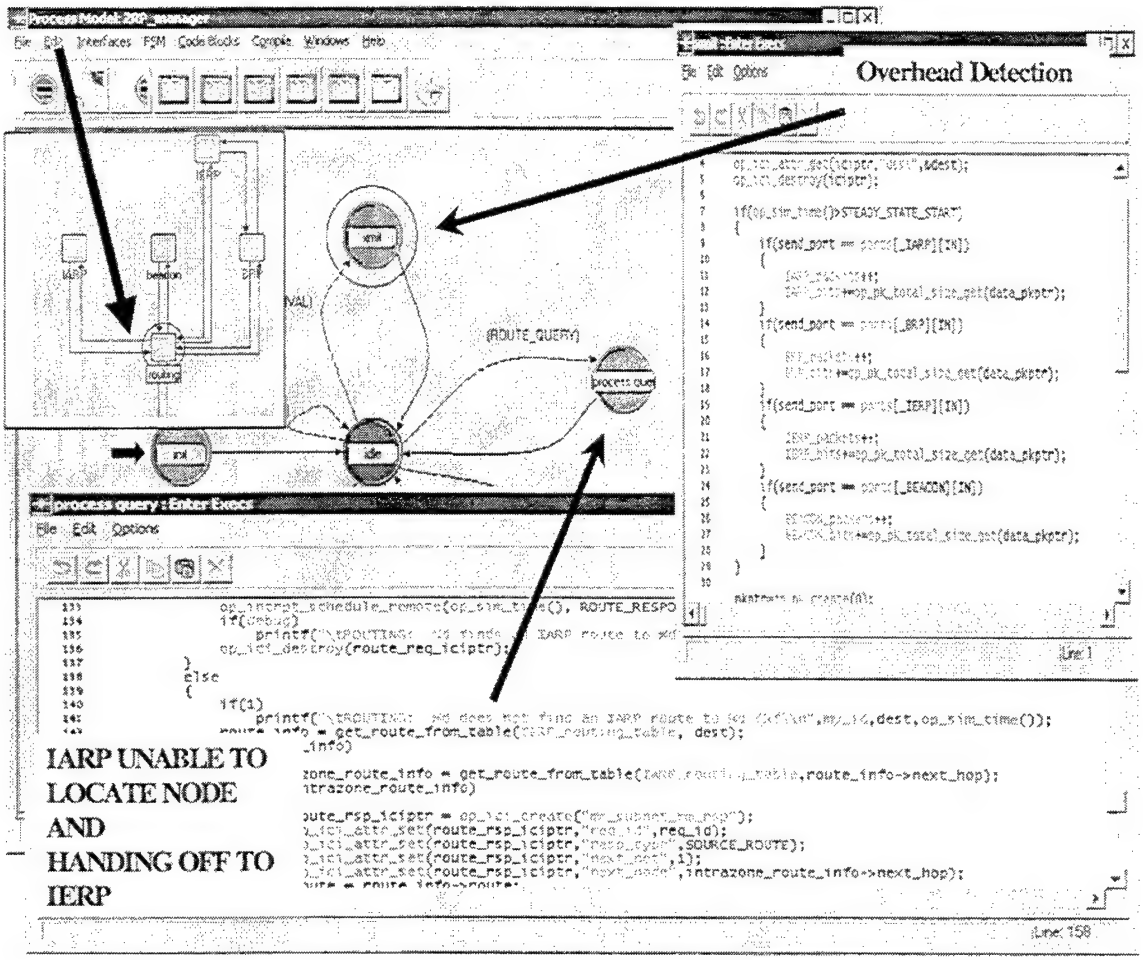

Figure 13. Depiction of Routing Node Object Within ZRP_Manager.

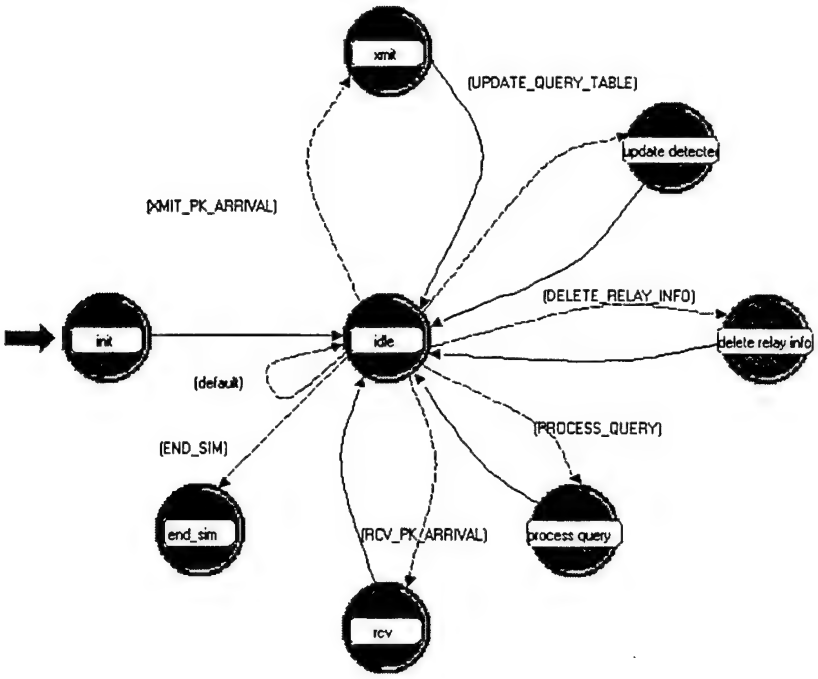

Figure 14. IARP Process Model.

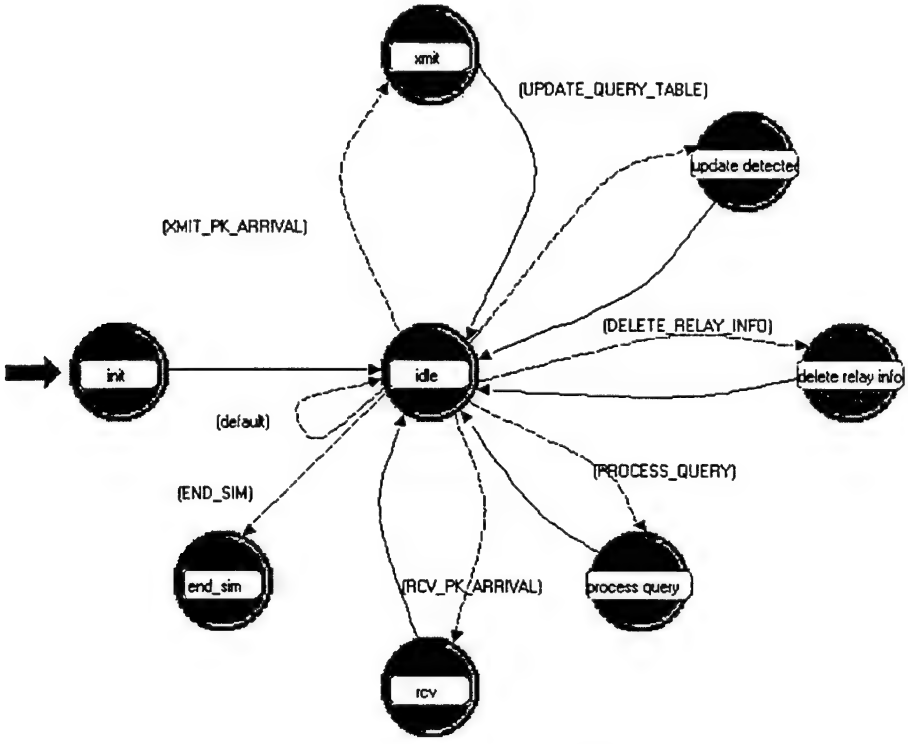

Figure 15. BRP Process Model.

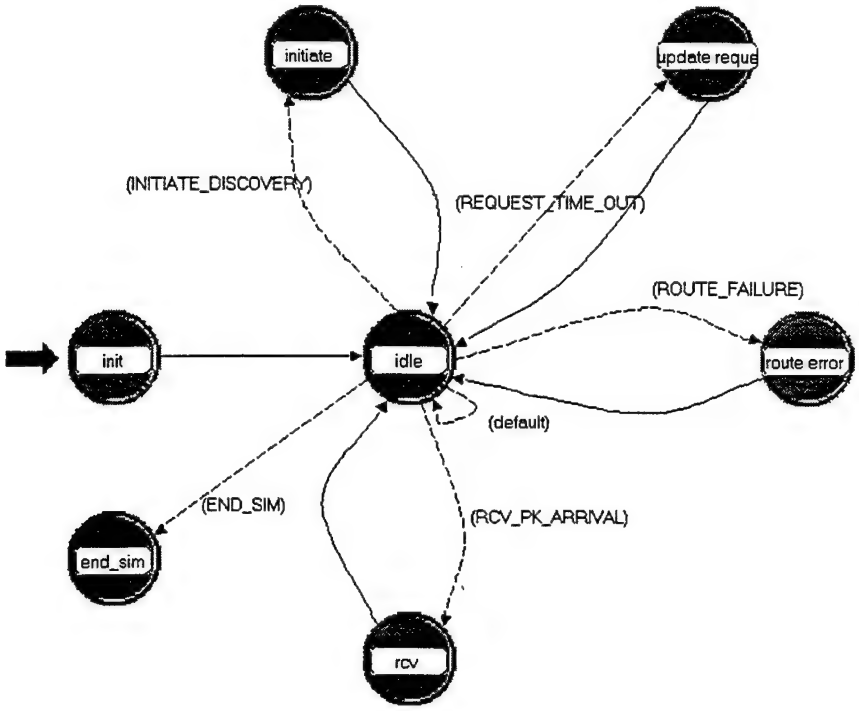

Figure 16. IERP Process Model.

The simulation traffic is controlled by the *model attributes* of the *app* process model depicted in Figure 17. The number of *total sessions* (transmissions per simulation), *packets per session*, *session interarrival delay*, *packet interarrival delay*, *mode* (transceiver pipeline model), and *destination*, are manipulated from this window. The destination of each session (transmission) is usually set using a uniform random variable for delivery throughout the network. A single session can be setup between two nodes if the time to execute a single session exceeds the simulation time. This is accomplished by increasing the *packets per session* until time of delivery exceeds the simulation time. The simulation is interrupted before another session with a MANET node is initiated. This traffic channel analysis is only beneficial when using complex transceiver pipeline modeling which will be explained in the following section.

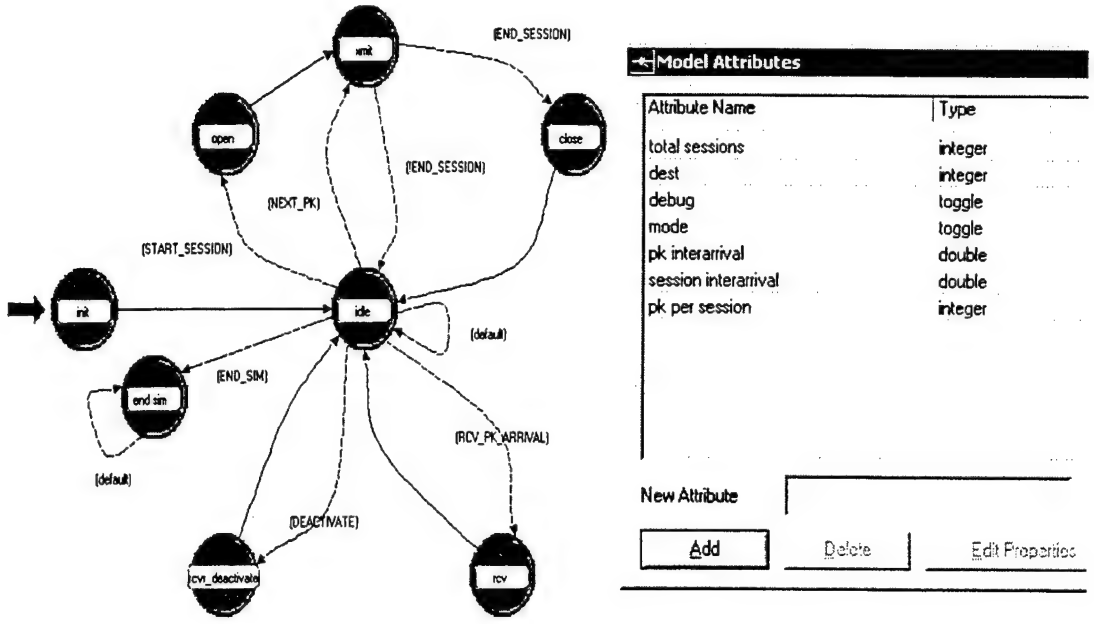

Figure 17. APP Process Model and Attribute Window.

2. LINK ESTABLISHMENT

OPNET simulates communication between two nodes through a process known as the *transceiver pipeline*. The *transceiver pipeline* models the transmission of packets across a communications channel (link). The OPNET package factors in the MAC layer attributes and includes multiple stages to model the channel's behavior. Both the radio transmitter and radio receiver node objects (*tx_simple* and *rx_simple* in Figure 12) include the following transceiver pipeline attributes: transmission delay, link closure (LOS), channel match, transmitter antenna gain, propagation delay, receiver antenna gain, received power, background noise, interference noise, signal-to-noise ratio (SNR), bit error rate (BER), error allocation, and error correction.

The complexity of the *transceiver pipeline* was intentionally bypassed in the current model to simplify the communication simulation between ZRP MANET nodes [14]. Each mobile node utilizes a transmitter and receiver in *direct delivery* mode. The *direct delivery* attribute bypasses the transceiver pipeline options resident in OPNET and provides error free delivery to the destination node. Packet delivery fails only if a node moves out of range. An error free transceiver pipeline is assured if a destination node falls physically within the source node's transmitter radius. The *delivery* node object handles this process through the *tx_simple* and *rx_simple* node objects depicted in Figure 12. The simple implementation of *tx_default* and *rx_default* alone does not enable

OPNET transceiver pipeline modeling. It was determined by the author that further code and model modifications are necessary to interface with the transceiver pipeline model mechanisms. As explained above, with code and OPNET model changes, more complex link analysis could be used to create ad hoc transceiver pipeline and traffic generation.

Inside the *delivery* node object, a *packet_delivery* process model provides the ideal MAC for the ZRP model [14]. The *beacon* module was specifically written for this simulation and handles neighbor discovery in a manner similar to most MAC protocols. The bits transmitted by the beacon module are not counted as overhead against the ZRP protocol since the MAC layer is present regardless of the protocol instituted. The *tx_default* and *rx_default* allow for future interaction with OPNET transceiver pipeline modeling. The channel attribute setting in both *tx_default* and *rx_default* can be manipulated to set data pipeline size. Due to an undetermined coding error in the ZRP model, 10 Mbps was used as the default *channel rate*. Troubleshooting indicated a pointer error caused by the function call, *update_Detected_Queries_Table*, which is depicted in Figure 18. The function call resides in *IERP* and is located in the *Enter Execs* of *update_request*. The corrective action taken was to comment the code out during execution and this was determined to not impact the model results with a 10 Mbps channel rate.

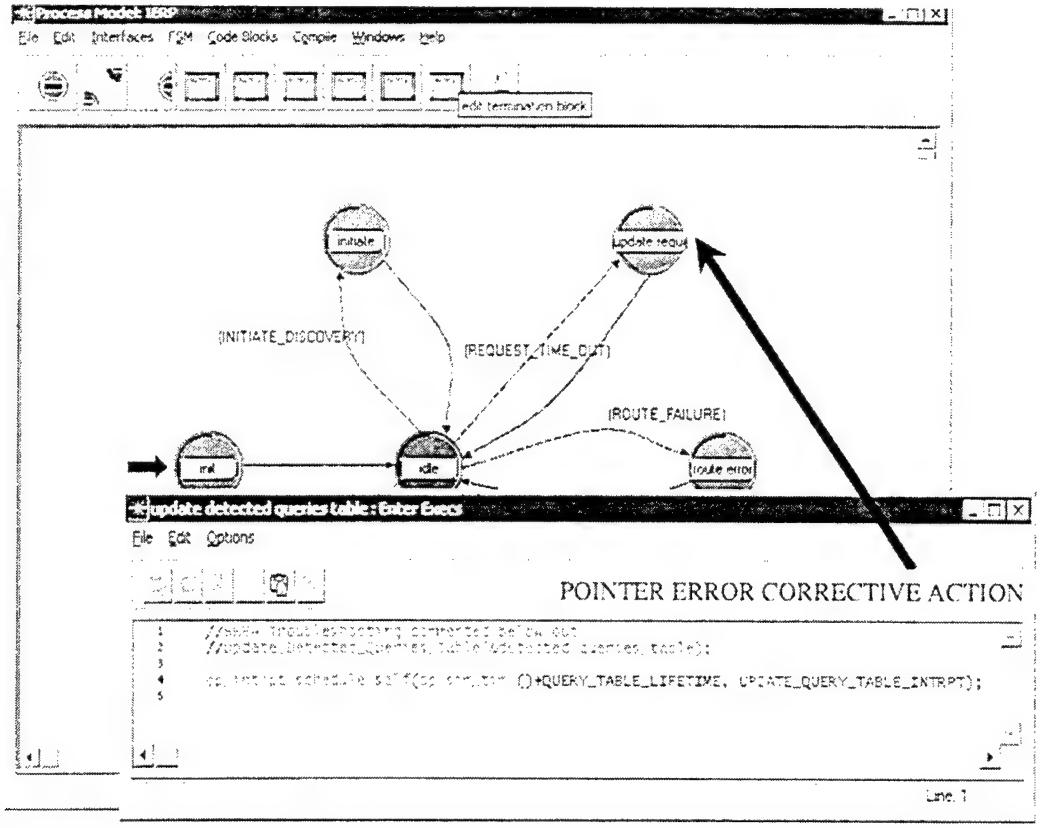

Figure 18. Pointer Error Correction to IERP Process Model.

3. NODE MOVEMENT

Node movement is simulated by the *move* node object depicted in Figure 12. As mentioned above, the user is able to input a uniform velocity in km/sec for all the MANET nodes from the simulation attribute window. At t = 0 sec, each node heads off on a direction assigned by a uniform random variable, in the range [0-2π], invoked by *move*. If a node impacts the edge of the virtual xy plane, it is detected by a transition condition in the *move process model*, a direction is recomputed in the range [0-2π], and the mobile node continues to move about the virtual x-y plane. The animation attributes of OPNET depicting this random movement by selecting *record animation* from the *project editor* menu. A viewer window, *m3_vuanim*, can be deployed by selecting *play animation* following the execution of a simulation to view the random node movements. *M3_vuanim* uses a tape recorder like interface that can be manipulated to control the speed of node movements.

4. STATISTICS PRODUCTION

Due to the cumbersome statistic collection methods of earlier versions of OPNET, a standard C code export file command, *fprintf*, was used in the ZRP model to collect statistics for analysis [14]. As the code executes, standard **.dat* files are produced in the OPNET *bin* folder at the conclusion of each simulation. As explained earlier, although OPNET has inherent statistical collection, the standard node objects were not utilized throughout the ZRP model, so there is no connection with the inherent statistical collection of OPNET. The technique employed by the ZRP model is to use static variables declared in the process model code to provide the basis to gather statistics. The various process models have *END_SIM* states, which gather statistics during each process model execution call by the ZRP model. Figure 19 depicts the *app* process model which contains the *END_SIM* state for statistic production. This information traffic meter was added to the latest ZRP version to provide visibility to data throughput and efficiency [14]. The *kevin_stat2* meter measured *sessions_sent*, *sessions_rcvd*, *packets_sent*, *packets_rcvd*, *bits_sent*, *bits_rcvd*, *total packet delay*, and *total jitter*. MATLAB was utilized to organize collected data and produce results for analysis. Previous work on the ZRP model focused on ZRP overhead and had elected to neglect the traffic parameters [14].

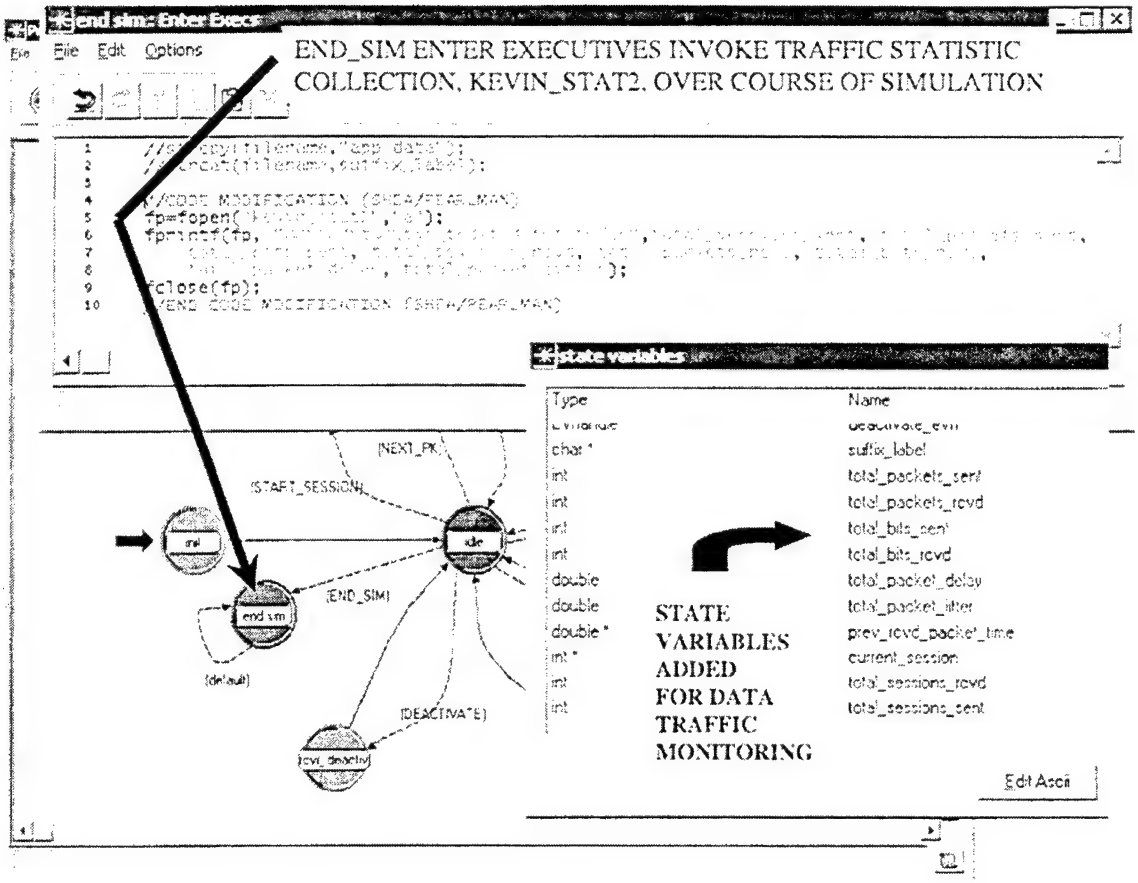

Figure 19. Example Of END_SIM Statistical Collection.

C. SUMMARY

This chapter has provided an introduction to OPNET Version 7.0 and presented the ZRP model which was converted to Windows NT from a UNIX implementation. OPNET uses the concept of *workspace*, *network models*, *node models*, *node objects*, and *process models* for network simulation. The behavior of mobile nodes using the ZRP protocol in a MANET environment is executed through the *manet_ls* node model. *Routing* routes traffic queries generated by the *app* process model to the appropriate *IARP*, *IERP*, and *BRP* process. Traffic delivery between nodes is ensured during each *session* (transmission) through the use of the *direct delivery* mode. Source traffic volume can be adjusted through the *app* attribute window. *Move* provides random movement and constant velocity to each node over the course of the simulation. Statistics were collected on each simulation through the use of the *fprintf* command executed in the *END_SIM* states of various process models and analyzed in MATLAB. A source traffic meter was added to the ZRP model for routing efficiency analysis.

V. RESULTS

In this chapter, the results of the ZRP OPNET simulations with the Marine scenario are analyzed. The focus of this analysis was to evaluate the efficiency and reliability performance of the protocol. As discussed in Chapter IV, due to the hardware limitations of the Windows NT platform, experimentation was required to determine simulation parameters which could be evaluated within hardware constraints. Section A explains the scenario and configuration development process to meet these limitations. Previous research results from Hass and Pearlman [4] are utilized to provide a comparison with the results from this work and also illustrate ZRP behavior which could not be demonstrated with the Marine scenario. The traffic overhead generated by ZRP is presented in Section B by component (IARP, IERP, and BRP) to better understand the contribution from each sub-protocol which shapes the behavior and efficiency in a MANET environment. The first case examines ZRP overhead with changing zone routing radius. The second case examines ZRP overhead with changing velocity. Section C utilizes the same two situations to study the link performance of ZRP in the Marine scenario. This chapter concludes with an analysis of efficiency and routing optimization. Efficiency is measured against link performance to better understand the tradeoff between routing overhead and link performance. Using the Marine scenario as a case study, results of the min-searching and traffic adaptive methods of routing optimization are presented.

A. SCENARIO

The network configuration used in this scenario was designed to mirror the tactical use of JTRS by individual Marines. JTRS will provide the next generation of tactical radios for the warfighter. The network implementation was designed to emulate a Marine rifle platoon operating with a JTRS squad-level radio. Although a Marine rifle platoon operates with forty-two personnel, thirty-two nodes were utilized in this work, which provides a reasonable representation of this combat force. The number of nodes was kept to thirty-two to reduce the demand on the Windows NT platform's limited computing power and to reduce simulation time. The 32 MANET nodes, modeled by the process model *manet_ls*, represent individual Marine rifleman with individual movement and data exchange capabilities. In a rapidly developing combat situation, each Marine would transmit and receive information to his fellow Marines for control and situation

awareness. As explained in Chapter IV, each MANET node moves individually across the x-y plane and communicates in a random fashion to mimic combat maneuvering and tactical data traffic. It is important to note that due to the limitations of the current ZRP configuration, the MANET nodes do not move in tactical formations. Each node is an independent random variable for both movement and traffic placed on the net.

The *x_axis* and *y_axis* parameters for the simulation were configured to establish a 1 km × 1 km x-y plane to represent an operational area assigned to a rifle platoon. As depicted in Figure 11, the MANET nodes were placed in a checkerboard fashion from the OPNET *network editor* window. From repeated experimentation with simulation parameters, it was determined that a 1 square-kilometer x-y plane produced a node density that balanced the requirement for freedom of movement and mobile node interaction. As explained in Chapter IV, each MANET node moves at a constant velocity in km per second. However, a platoon will not intentionally disengage from each other and will seek to preserve their tactical formations. In order to facilitate this behavior, the *x_axis* and *y_axis* parameters restricted movement to preserve unit integrity, command and control, and combat power. Experimentation further demonstrated that the 1 square-kilometer maneuver space served the purpose of preserving an average node neighbor density between 3 - 5 neighbors during the simulation with transmit radius $t_r = 0.2$ km, as depicted in Figure 20.

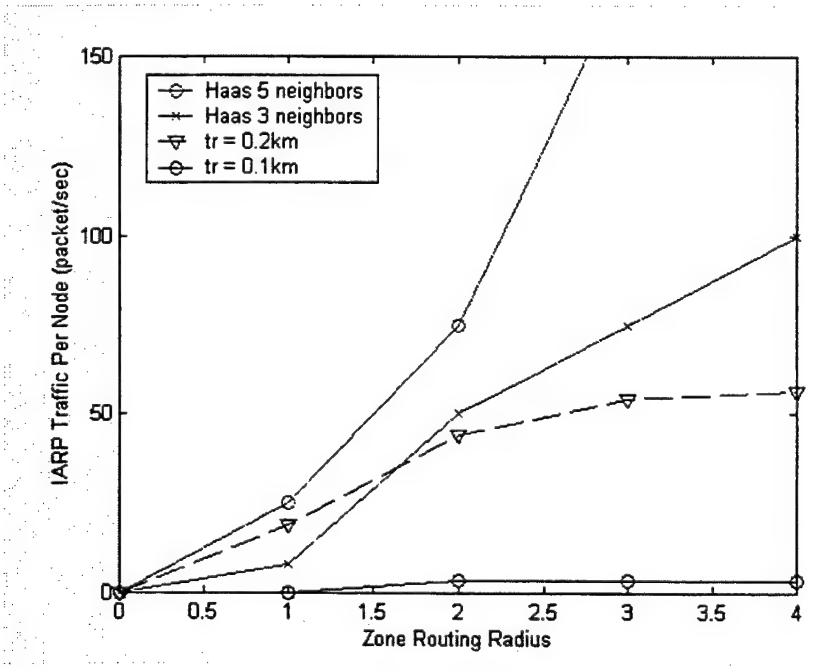

Figure 20. IARP Overhead with Changing Zone Radius (After Ref. [4]).

In order to provide a model reference and measure the amount of neighbor density driven by the scenario at various t_r and ρ settings, the comparison between IARP traffic per node and average neighbor density was accomplished by utilizing Ref [4], which measured the IARP packets per node and related it to neighbor density. Neighbor density, the number of MANET nodes that a source node can reach in one hop, is primarily a function of transmit radius. Neighbors impact the population of a source node's routing zone which dictates the amount of IARP traffic. The IARP meter, explained in Chapter IV, provides the feedback on each source node over the course of the simulation. From the data produced from the IARP meter, Figure 20 was produced to measure the average neighbors per node and IARP traffic per node (packets/sec). Figure 20 illustrates the Marine scenario with $t_r = 0.2$ km and $t_r = 0.1$ km compared with more dense ZRP simulations and larger x-y planes. As depicted, $t_r = 0.2$ km provided between 3 and 5 neighbors at zone routing radius of $\rho = 1$. For $\rho > 1$, the IARP traffic per node approaches a peak of 50 packets/seconds. This leveling effect is due to the small network size. As the ρ increases, its impact on the network is limited due to the small size of the network. With $t_r = 0.1$ km, the IARP traffic was reduced due to with decreased neighbor density as a result of a smaller transmit radius. Simulation at $t_r = 3$ km proved to be impractical for the Windows NT platform being utilized due to exponential simulation time increases as ρ was increased. As shown in Figure 20, the IARP traffic increases considerably as node density and ρ are increased in conjunction. The data points from Ref [4] in Figure 20 are provided to illustrate this behavior of ZRP in a MANET with a higher level of neighbor density that could not be modeled due to hardware limitations.

Figure 21 illustrates the random movement of the nodes over the course of a typical simulation. The hollow circles depict the checkerboard starting positions displayed in Figure 11. At the conclusion of the simulation, the MANET node positions are recorded by the stars. From the final positions, clusters of nodes and network partitions are clearly visible. When MANET nodes cluster, the network is enhanced through multiple transmission routes. However, on the outer edges of the network, mobile nodes lack network stability and form a network partition which is completely cut off from the rest of the network.

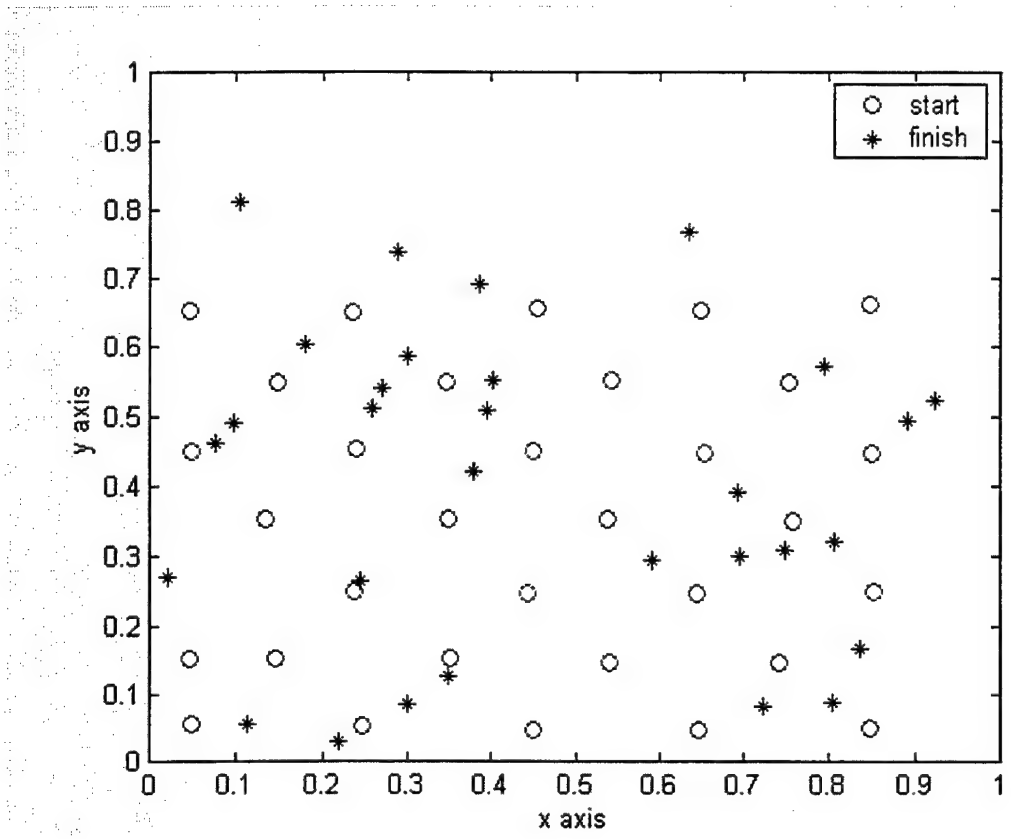

Figure 21. Typical Scenario Movement Results.

1. Configuration

The ZRP model provided to the author was developed using earlier versions of OPNET (Versions 3.5 – 6.0) in a UNIX environment. As a result, the model had to be updated to OPNET Version 7.0 and some code changes had to be made to facilitate the implementation on a Windows NT platform. For instance, the variable M_PI is used by UNIX to represent the constant π and was not recognized by the Microsoft Visual C++ compiler linked with OPNET running on the Windows NT platform. The OPNET kernel procedure *op_mko_all* was used to force the conversion to Version 7.0. Multiple code modifications were required to manipulate the ZRP versions, code, and process models to achieve proper execution of the simulation. The most recent version of the OPNET ZRP model was utilized. This included the new IARP process model, *IARP_ls*, which executes a purely periodic proactive routing protocol.

As explained in Section A, IARP traffic is directly related to node density and proved to be the pivotal barometer which established the scenario parameters that could

be modeled on the Windows NT platform for this analysis. A zone routing radius of $\rho > 1$, *x_axis* = 1 km, *y_axis* = 1 km, and a transmit radius of $t_r \leq 0.3$ km resulted in a reasonable IARP OPNET simulation event list requirement by tempering the neighbor density. Due to a programming decision, $\rho = 0$ cannot be directly entered into the simulation parameters of the ZRP model [14]. The ZRP model implementation requires a simulation parameter of $\rho = 1$ to simulate the $\rho = 0$ state. Therefore, ρ settings must be incremented by one in simulation window entry. The next version of ZRP will allow for a $\rho = 0$ entry. The neighbor density was determined to be acceptable at a transmit radius $t_r \leq 0.3$ km and a simulation time of 15 minutes. The routing zone radius was kept at $\rho \leq 4$ due to unreasonable simulation times above this threshold. The *sessions per transmission* (data transfers per transmission) was set to 1 to decrease transmission load. Session interarrival was not a factor in this case. Packet size is 1,000 bits and one packet was sent during each *session* (transmission). Since only one packet was transmitted per session, packet interarrival delay was not modeled. The channel data rate was set for a default 10 Mbps due to a memory error at lower data rates (see Link Establishment, Chapter IV for details). Based on the simulation parameters explained above and experimentation, it was determined that scenario simulation times were limited to 15 minutes to keep OPNET simulation time to approximately 3 hours. For instance, OPNET required 2 days to simulate the Marine scenario with $t_r = 0.5$ km, $\rho = 3$, and scenario simulation time of 15 minutes.

B. OVERHEAD GENERATION

From Chapter IV, the overhead generated by the ZRP was monitored by an overhead traffic meter placed in the process model of *zrp_manager*. Figure 22 illustrates the overhead generated by ZRP in bits/sec per MANET node over a 15 minute simulation of the Marine scenario with $t_r = 0.2$ km, $v = 0.2$ km/hr, *x_axis* = 1 km, *y_axis* = 1 km, and ρ incremented from 0 to 4. Overhead is considered to be all IARP, IERP, and BRP data generated to provide routing functionality. IARP overhead is generated to provide in-zone routing and IERP/BRP is generated to provide out-of-zone routing. BRP overhead is equivalent to out-of-zone query requests due to its bordercasting and optimization role. IERP overhead is generated by route replies and route failure messages. As depicted in Figure 22, with a constant uniform node velocity and average neighbor density (primarily

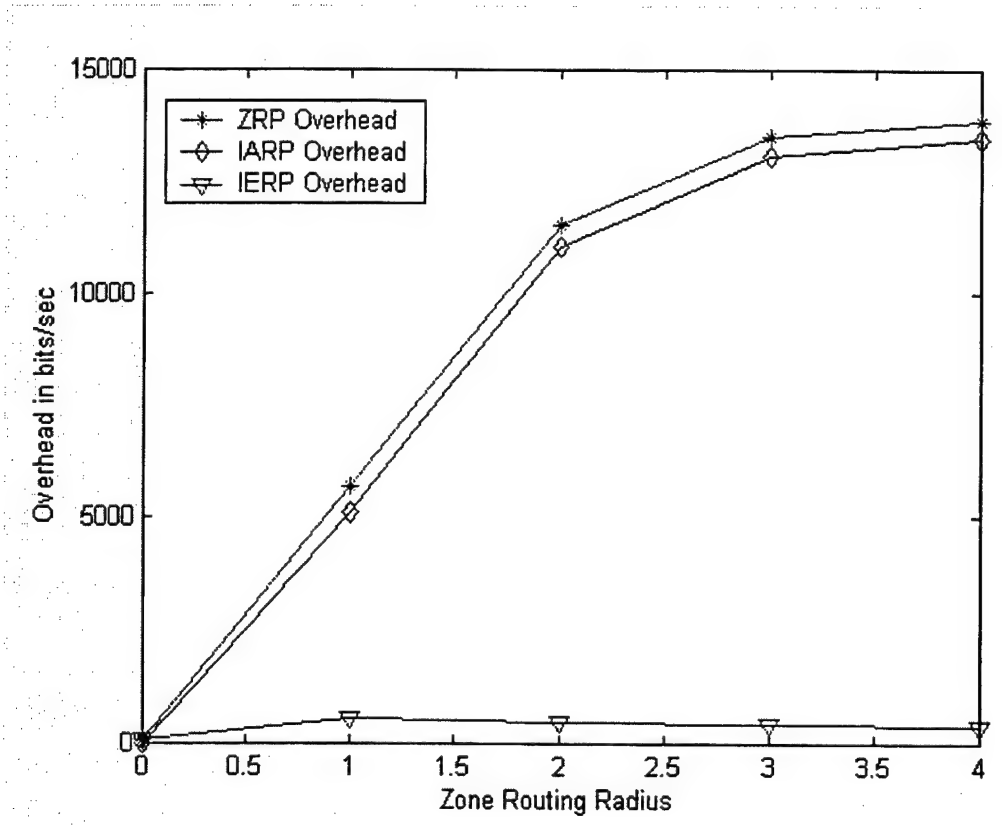

Figure 22. ZRP Overhead With Changing Zone Radius.

dictated by transmit radius), the zone routing radius is the critical parameter dictating the amount of ZRP overhead that is generated. In this figure, the proactive routing overhead associated with IARP quickly increases as ρ is expanded. IERP overhead in bits/sec remains relatively constant and slowly declines as ρ is expanded. The low IERP overhead at ρ = 0 is dictated by traffic generation among MANET nodes [14]. An increase in traffic query demands would dictate an increase of IERP overhead at ρ = 0. IERP overhead steadily declines with increasing ρ as the IARP zone routing is able to respond to route query requests with its large route cache due to a large reactive routing zone.

Figure 23 is used to illustrate the behavior of ZRP overhead (packets/sec) generated per node with increased zone routing radius. The zone radius that minimizes ZRP overhead can be experimentally determined. The simulation parameters for the Marine scenario are t_r = 0.2 km, ν = 0.2 km/hr, *x_axis* = 1 km, *y_axis* = 1 km, and ρ is incremented from 0 to 4. The Marine scenario is measured against Haas results to better depict the "U" shape of ZRP overhead in regions outside the capability of this scenario. At ρ = 0, ZRP overhead is driven by IERP packets per second required to meet traffic

requirements since IARP overhead is zero packets/sec in this region (see Figure 9). In Figure 22, as ρ increases, IARP overhead increases with zone routing radius. IERP overhead as a percentage of ZRP overhead is reduced due to the reactive zone cache built from proactive IARP routing. The result is an overall decrease in ZRP overhead as shown in Figure 23. As ρ continues to increase, IARP overhead traffic rises exponentially. As Figure 22 illustrates, IERP overhead continues to increase in this region due to link instability, but at a much slower rate when compared to IARP overhead.

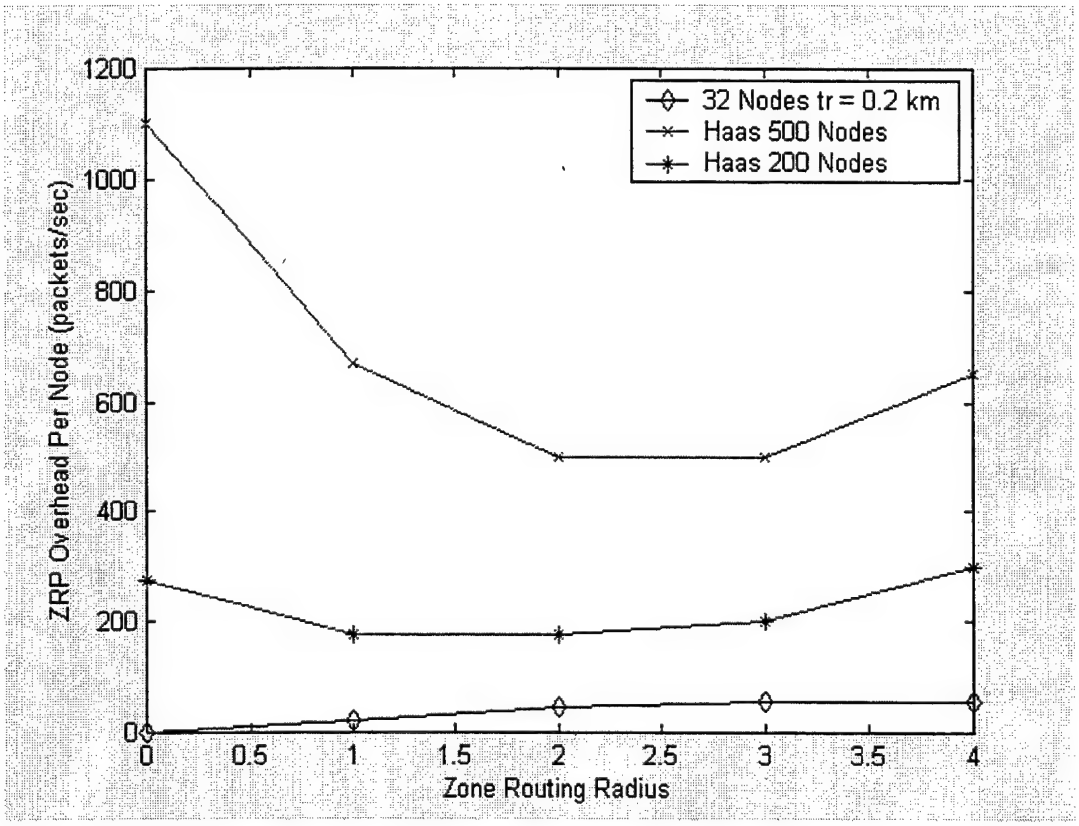

Figure 23. ZPR Traffic Per Node (After Ref. [4]).

In addition, Figure 23 indicates that the Marine scenario does not show the downward trend in ZRP overhead per node. This is due to the low traffic generation rate and small scale of the MANET environment simulated by the Marine scenario to remain within hardware limitations. The Marine scenario also does not show a sharp rise in ZRP overhead as ρ increases and this is due to the limited number of MANET nodes. The ZRP overhead in the Marine scenario reaches a plateau of IARP traffic generation by ρ = 4. The Haas scenarios of 500 and 200 node simulations are provided to illustrate this

behavior which could not be simulated. As ρ increases, more nodes are added to the zone, thus increasing the amount of IARP packets/sec per node. This example also serves to illustrate the earlier point that ZRP behavior is shaped by the MANET environment itself and ZRP performance will differ between MANET simulations.

Figure 24 illustrates the advantage of a hybrid MANET protocol with respect to changing velocity. The simulation parameters used for the Marine scenario were $t_r = 0.2$ km, $\rho = 2$, *x_axis* = 1 km, *y_axis* = 1 km, and v is incremented from 0 to 0.8 km/hr. IARP is designed to be timer based and independent of event triggers (neighbor

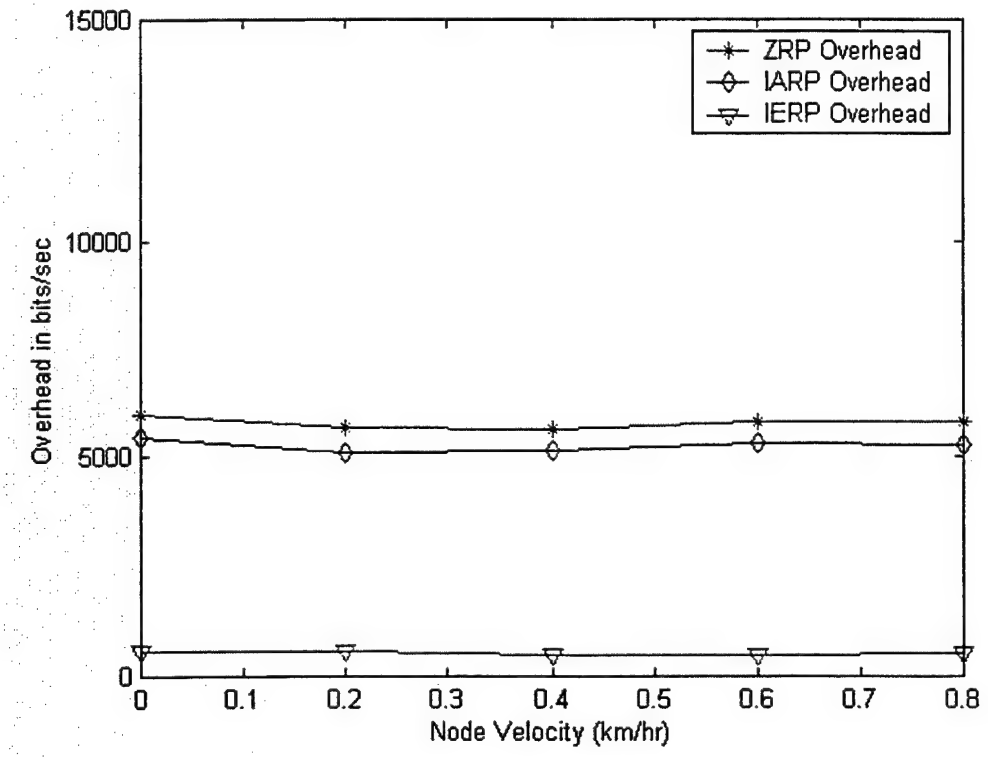

Figure 24. ZRP Overhead With Changing Velocity.

discovery/neighbor loss). This is why the version of the time triggered IARP process model, *IARP_LS_timer*, utilized was critical. As depicted in Figure 24, the ZRP overhead remains relatively constant over the course of the simulation. The fluctuation is due to IERP that is impacted by node velocity, traffic generation, and link stability. IERP is responsible for maintaining routes during transmissions (*sessions*). The IERP variance is low since the simulation limited the number of packets/session in the configuration. With a large data channel, 10Mbps, the IERP route repair occurrences remained low. A

simulation with longer transmissions (*sessions*) with a smaller data channel rate between MANET nodes would have caused a rise in ZRP overhead. In this situation, the IERP overhead would force the curve upward due to the need to reestablish links, which were broken due to node mobility. The result is that ZRP overhead to support a MANET environment is independent of node velocity.

C. LINK PERFORMANCE

Figure 25 is provided to depict the link performance of ZRP as the zone routing radius is increased. A result reported by Haas is compared to the Marine scenario to provide scale with a larger MANET simulation with a higher level of average neighbor density. The Marine scenario represents a 15 minute simulation of the 32 node network with t_r = 0.2 km, v = 0.2 km/sec, *x_axis* = 1 km, *y_axis* = 1 km, and ρ incremented from 0 to 4. The Haas scenario illustrates a simulation of 1000 nodes at average neighbor density equal to five [4]. As shown in Figure 25, there is a correlation between link failures/sec and ρ. The Marine scenario records approximately 0.75 failures/sec at $\rho = 0$ to approximately 0.62 failures/sec at $\rho = 1$. For $\rho < 1$, the failures/sec decrease steadily to 0.6 failures/sec. The flattening of the curve in the Marine scenario is due to the small scale of the network, which renders the routing zone increase less effective at large values. The decrease is a constant downward trend with network sizes of 1000 nodes and varies according to node density [4]. Node density, the average neighbors per node, is dictated by transmit radius and is not a function of ρ. The downward trend in failures is a result of routing zone expansion which provides increased reliability. The ZRP mechanism which increases reliability is BRP. Instead of having to route through each node to the destination, BRP provides an optimum routing mechanism which exploits available IARP link-state information in each routing zone for optimization, thus decreasing hop count to destinations. The Haas example illustrates the impact of neighbor density that amplifies the routing optimization, which can be achieved from the proactive routing zone cache of IARP. Neighbor density is increased by increasing transmit radius of each MANET node. There is a difference of approximately 0.1 failures/sec between the two cases until $\rho = 2$. This decreases the potential for link failure (route unable to be established) due to node movement, channel interference, and other factors associated with links between nodes. As a result of using ZRP, the link performance increases as the zone routing radius is increased.

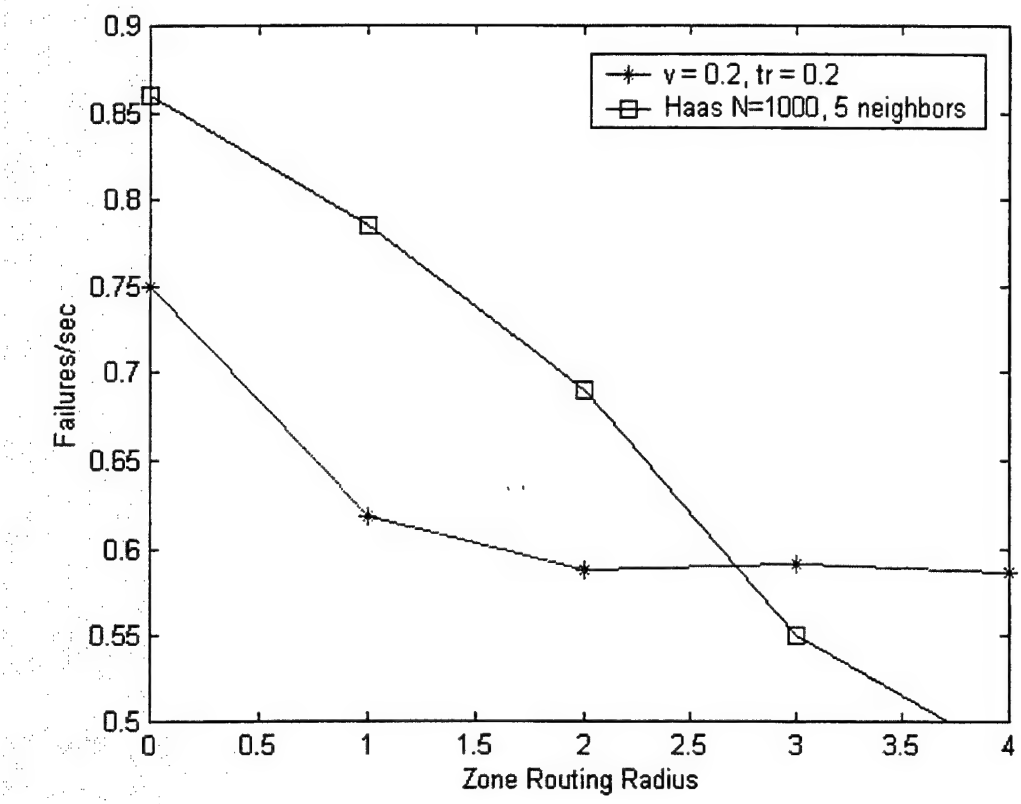

Figure 25. Link Failure Percentage With Increasing Zone Routing Radius (After Ref. [4]).

The purpose of Figure 26 is to evaluate the impact of velocity on link performance with ZRP if the zone routing radius is held constant. The simulation parameters used with the Marine scenario for Case 1 were t_r = 0.2 km, ρ = 2, *x_axis* = 1 km, *y_axis* = 1 km, and v was incremented from 0 to 0.8 km/hr. At ρ = 0, the link failure percentage of the Marine scenario was approximately 57%. As the zone routing radius was increased, the failure percentage continued to rise. An increase in node velocity decreased the ability to maintain route stability. The time to transmit a message over the link becomes a problem due to shorter periods of route stability with increased node mobility. The deviation from this upward trend at v = 0.8 km/hr was unexpected. A repeat simulation with a different seed value, Case 2 on Figure 26, did not produce a large variation from the previous simulation. When the simulation was repeated at a lower neighbor density, Case 3 (transmit radius t_r = 0.1 km), inconclusive results were observed. The link failure rate hovers at 95% with no distinct trends. The link failure percentage was expected to have increased with velocity in both situations. This does occur in both Case 1 and Case 2 until an anomaly at 0.8 km/hr. Case 1, with transmit radius t_r = 0.1 km, does not echo

this trend. At $v = 0$ km/hr, the link failure percentage is 94.66% and does rise to 96.22% at $v = 0.6$ km/hr. However, there is a decrease in link failure percentage at $v = 0.4$ km/sec. The Marine scenario fails to produce a distinct ZRP behavior.

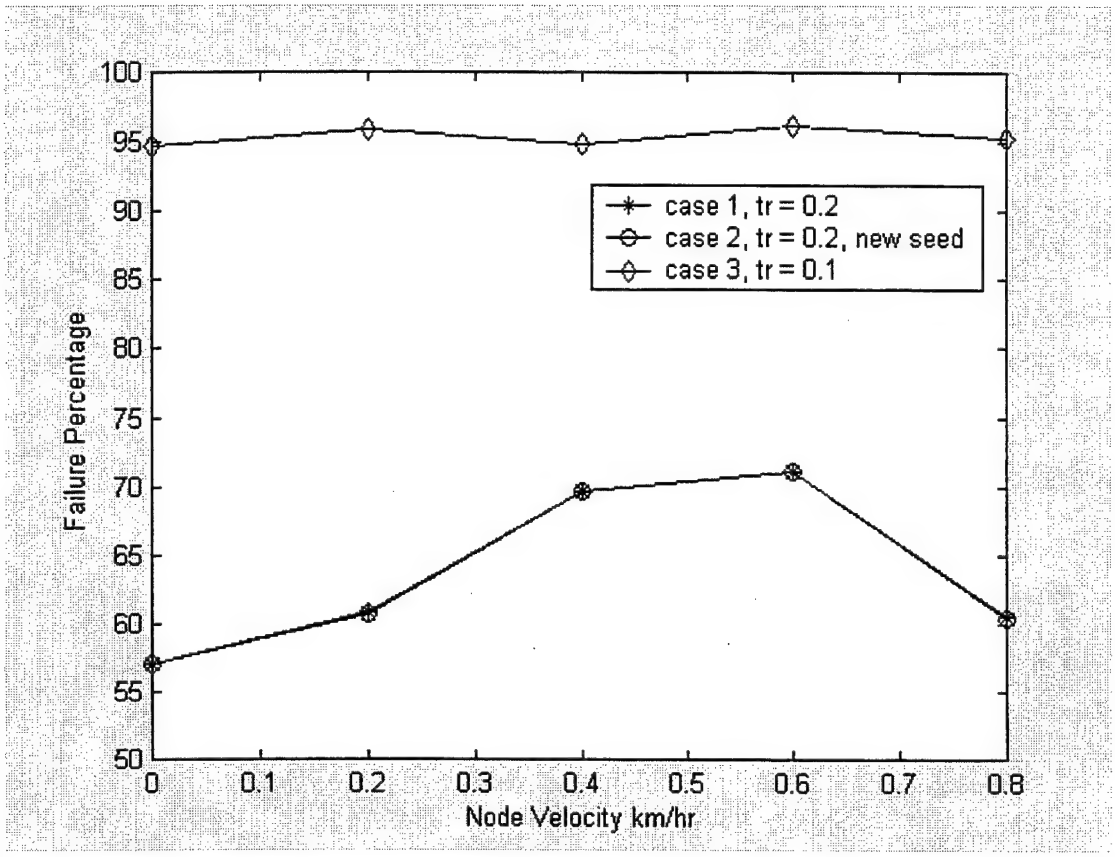

Figure 26. Link Failure Percentage With Changing Velocity: Case 1, 2, and 3 With $\rho = 2$.

D. EFFICIENCY AND OPTIMIZATION

An important goal of this thesis was to look at the efficiency of this algorithm. Efficiency (η) was measured as follows:

$$\eta = I / (I + OH)$$

where I is the amount of information data bits and OH is the amount of overhead bits. At $\rho = 0$, ZRP is producing minimal overhead and is at maximum efficiency. As the zone routing radius increases, ZRP overhead increases rapidly due to IARP overhead which quickly decreases the efficiency. However, due to the small size of the Marine network, the decay quickly reaches a steady state. Figure 27 displays efficiency and link

completion percentage as a function of zone routing radius and depicts the tradeoff between efficiency and link performance. As discussed earlier, the ideal zone routing radius is when IERP and IARP traffic are balanced. From this diagram, from a pure efficiency standpoint we can determine that the ideal zone routing radius would be $\rho = 1$. This zone routing setting would provide the least amount of inefficient routing with a large link completion percentage. All values of zone routing radius greater than 1 provide a marginal increase in link completion along with a decrease in routing efficiency.

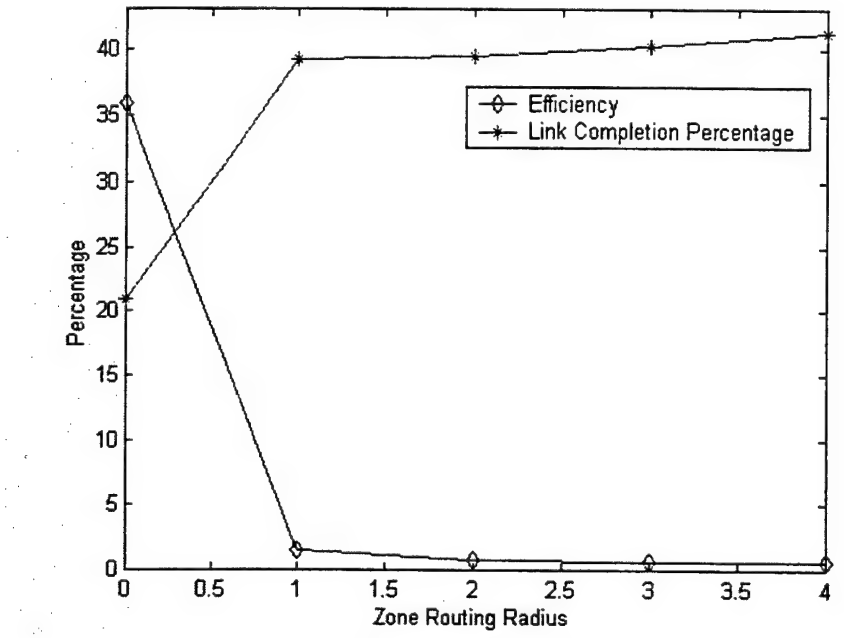

Figure 27. ZRP Data Efficiency.

In accordance with the ZRP min-searching and adaptive traffic method of routing optimization discussed in Chapter III, the optimal setting for the Marine MANET environment would be $\rho = 1$. Figure 28 displays routing zone optimization using the measurements at each interval. IERP only dominates in the $\rho = 0$ setting, where the ratio of IERP overhead to IARP overhead (IERP/IARP) goes to infinity since IARP traffic is 0. The closest setting to achieving balance between IERP and IARP traffic is at $\rho = 1$. The min-searching method assumes that the traffic of each node does not change drastically over time and would determine ρ_{opt} in the following manner. Figure 22 is more applicable to this method. As depicted in Figure 22, starting at $\rho = 0$, the IERP traffic and IARP traffic are both on the rise. The undershoot situation is realized with IERP traffic increasing. At $\rho = 1$, both IARP and IERP are increasing; this would be determined as an

undershoot region. For $\rho > 1$, IERP is decreasing and IARP is increasing which points to an overshoot situation. Therefore, $\rho_{opt} = 1$ is forced by the adaptive traffic method.

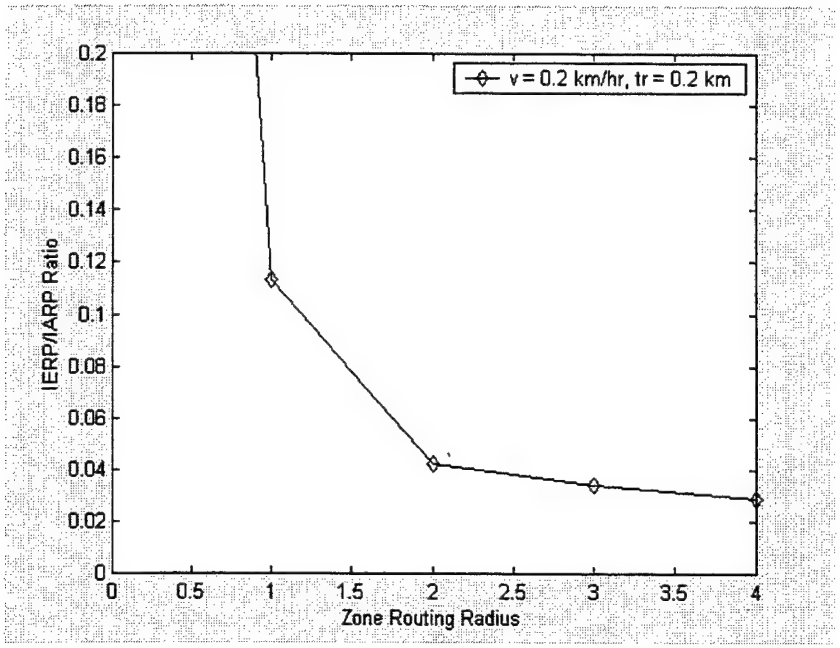

Figure 28. IERP/IARP Routing Zone Optimization.

E. SUMMARY

The Marine scenario configured for this analysis was hampered by a Windows NT platform which could only support 32 MANET nodes with an average neighbor density of 3-5 nodes. The Marine scenario failed to demonstrate the complete behavior of ZRP when compared to the results reported by Hass [4]. This echoes the point that ZRP behavior will be different in various MANET environments. The overhead traffic generated by ZRP was broken down into component (IARP, IERP, and BRP) traffic. IARP overhead traffic provides the majority of routing traffic as the zone routing radius is increased. The amount of IARP traffic is a function of node neighbor density. The "U" shape behavior of ZRP overhead per node was not realized in the Marine scenario. The amount of traffic generated by the limited number of MANET nodes was not sufficient to mirror this behavior. ZRP proved to be relatively independent of velocity in the Marine scenario. Due to the low traffic generation rate, the variation in IERP overhead traffic was minimal. The ability to communicate does improve as the zone routing radius is increased. However, this effect became minimal at large zone routing radius values in the Marine scenario. The effect of changes in velocity on MANET nodes running ZRP

proved to be inconclusive. Despite varying the average neighbor density, no distinct behavior was identified. In the Marine scenario, $\rho = 1$ was proved to be the optimal zone routing radius by the min-searching and traffic adaptive methods. There was a distinct tradeoff between routing efficiency and link performance when adjusting the zone routing radius.

VI. CONCLUSIONS AND RECOMMENDATIONS

A. CONCLUSIONS

The results of this thesis provided a snapshot into the performance of ZRP in a small generic mobile ad hoc network chosen to represent a future JTRS architecture on the relative scale of a single Marine rifle platoon operating in a 1 square kilometer area of operation. The complete behavior of ZRP was not demonstrated in the Marine scenario due to the limited number of nodes (32), the low traffic generation , and the small x- and y-axis boundaries due to performance limitations of the Windows NT platform. Previous results reported by Haas and Pearlman were used as a rheostat to scale the results from the Marine scenario to the behavior of ZRP in that of a much larger network with MANET environment parameters outside of the capabilities of this work.

The traffic overhead behavior of ZRP in the Marine scenario was consistent with a hybrid MANET protocol. With constant velocity and average neighbor density (primarily dictated by transmit radius), the zone routing radius proved to be the critical parameter dictating the amount of ZRP overhead generated in the Marine scenario. IARP overhead traffic increased rapidly as the zone routing radius is increased. The small size of the network forced the IARP traffic increase to level off when it would otherwise continue to increase in a larger network with greater neighbor density. IERP traffic overhead is driven by the traffic generation of the source nodes. IERP overhead traffic caused ZRP overhead fluctuations in the presence of changes in velocity. IERP is responsible for repairing routes, and this activity is slightly increased as a result of route instability introduced by velocity. However, the periodic behavior of IARP is independent of node velocity and was unaffected by adjustments to node velocity with the Marine scenario.

ZRP link performance was improved in the Marine scenario by increasing the zone routing radius. When compared to previous research, a decrease is more continuous with network sizes of 1000 nodes and varies according to node density [4]. The variations in neighbor density could not be effectively measured due to the limitations with the Windows NT platform. The increase in link performance was diminished due to the small scale of the network simulation, which rendered the zone routing radius increase less effective at large values. The link performance of ZRP appears to be directly related to node velocity in the Marine scenario. However, the results were inconclusive. In general, as the node velocity increases, the ability to maintain link

stability decreases. The time to transmit a message over the link becomes a problem with increased velocity due to short periods of route stability.

In accordance with the min-searching and traffic adaptive method of routing optimization, the optimal setting for the Marine MANET environment would be $\rho = 1$. IERP only dominated in the $\rho = 1$ setting where the ratio of IERP/IARP goes to infinity since the IARP traffic is zero in this region. The closest setting to achieving balance between IERP and IARP traffic is at $\rho = 1$. The Marine scenario demonstrated that ZRP is able to adapt to MANET environments through adjustments to the zone routing radius. Analysis relating link completion with zone efficiency produced an intersection point prior to the optimum zone radius. In the Marine scenario, the small size of the network produced flat curves once the zone routing radius exceeded 1. However, this technique may prove to be unreliable in a larger network since network performance and network efficiency would continue to rise and fall, respectively.

B. RECOMMENDATIONS

The scenario configured for protocol analysis is critical to accurately model a MANET protocol's behavior. Future studies of ZRP or other MANET protocols should incorporate simulations that are able to model a larger set of MANET nodes in a larger x-y plane. The author suggests using at least 100 nodes or more. Neighbor density level limitations due to computer hardware should reduced for future research. A small network was not sufficient to model all aspects of ZRP behavior. Traffic generation from the MANET nodes should be elevated to better model the IERP overhead behavior for small zone routing radius values. The larger traffic flow will also provide better feedback on the behavior of ZRP in regions of changing velocity. During each session (transmission), multiple packets should be transmitted to provide data on packet interarrival delay over the MANET network. The data rate of the channel should be reduced significantly to resemble more realistic levels. Third generation cellular networks will have 2 Mbps throughput. Marine Corps tactical radios currently are only capable of 9.6 kbps.

The ZRP OPNET model utilized in this work does not incorporate several important MANET environment factors in its current form. Power levels, ad hoc traffic, formation movements, transmit radius, and ad hoc velocity would more accurately model the military battlespace for JTRS implementation. Battery power remains a critical concern to the tactical radio operator. The IARP process should be modified to

incorporate a low power indicator for each mobile node. The BRP should be able to leverage this proactive data in the route optimization process. The node movement should be modified to create association, so groups of nodes could move about the battlespace. This group behavior would further improve the capability of the ZRP protocol. The group behavior would provide more consistent neighbors throughout the simulation and mirror real world tactical formations. Furthermore, the speed of each node or groups of node should be made ad hoc to further enhance the realization of the tactical scenario. Vehicle, foot mobile, helicopter, and aircraft traffic could be represented by varying the velocity of some nodes. Ad hoc transmit radius capabilities would provide a more realistic battlespace model. Foot mobile traffic would carry limited range squad radios. Vehicles, helicopters, and aircraft would have significantly larger ranges and bridge the battlespace.

ZRP is a simple hybrid MANET protocol that has a great deal of potential for JTRS. However, more in depth study and analysis is required to explore its capabilities. Comparison of ZRP with other MANET protocols over identical simulations should provide the level playing field for evaluation. It is hoped that this thesis has provided insight into the ZRP protocol and its potential application to a small ad hoc mobile network operating in a tactical environment.

THIS PAGE INTENTIONALLY LEFT BLANK

LIST OF REFERENCES

1. Operational Requirements Document (ORD) for Joint Tactical Radio System (JTRS), JTRS Joint Program Office, 23 March 1998.

2. Corson, Scott S., Macker, J., "Mobile Ad Hoc Networking (MANET): Routing Protocol Performance Issues and Evaluation Considerations," RFC 2501, January 1999.

3. Vaidya, Nitin H., "Mobile Ad Hoc Networks; Routing, MAC, and Transport Issues," MobiComm Tutorial, 15 July, 2000, pg 1- 431.

4. Haas, Zygmunt J., Pearlman, Marc R., "Determining the Optimal Configuration for the Zone Routing Protocol," *IEEE Journal on Selected Areas in Communications*, Vol 17, pg 1-16, August 1999.

5. Gerla, M., Lee, S. J., Toh, C. K., "A Simulation Study of Table-Driven and On-Demand Routing Protocols for Mobile Ad Hoc Networks," *IEEE Network*, Vol 13 Issue 4, pg 48-54, Jul-Aug 1999.

6. Maatta, Risto, "Wireless Ad Hoc Routing Protocols, a Taxonomy," Defense Forces Research Institute of Technology, Electronics and Information Technology Seminar, pg 1-19, 11 May 2000.

7. Misra, Padmini, "Routing Protocols For Ad Hoc Mobile Wireless Networks," Computer and Information Systems Paper 788-99, Ohio State University, 18 November 1999.

8. V. Park and M.S. Corson, "Temporally-Ordered Routing Algorithm (TORA) Version 1 Functional Specification," Internet Draft, draft-ietf-manet-tora-spec-00.txt, Dec 1997.

9. Lesiuk, Camberon B., "Routing in Ad Hoc Networks of Mobile Hosts," Directed Study, Department of Mechanical Engineering, University of Victoria, Victoria BC, Canada, 2 December 1998.

10. Johnson, David B., "Routing in Ad Hoc Networks," *Proceedings of IEEE Workshop*, pg 1-4, 1994.

11. Haas, Zygmunt J, Pearlman, Marc R., "The Zone Routing Protocol (ZRP) for Ad Hoc Networks," Internet Draft, draft-ietf-manet-zone-zrp-02.txt, June 1999.

12. Haas, Zygmunt J, Pearlman, Marc R., "The Zone Routing Protocol (ZRP) for Ad Hoc Networks," Internet Draft, draft-ietf-manet-zone-zrp-02.txt, June 1999.

13. Haas, Zygmunt, "A New Routing Protocol For The Reconfigurable Wireless Networks," pg 652 - 566, *IEEE Journal on Selected Areas in Communications*, Vol 12, October 1997.

14. Telephone conversation between Pearlman, Marc R, and the author, August 2000.

15. Advanced OPNET Modeler 7.0 Training Manual, OPNET Technology Inc., August 2000.

THIS PAGE INTENTIONALLY LEFT BLANK

INITIAL DISTRIBUTION LIST

1. Defense Technical Information Center 2
   8725 John J. Kingman Road, Ste 0944
   Fort Belvoir, VA 22060-6218

2. Dudley Knox Library 2
   Naval Postgraduate School
   411 Dyer Road
   Monterey, California 93943-5101

3. Director, Training and Education 1
   MCCDC, Code C46
   1019 Elliot Rd.
   Quantico, Virginia 22134-5027

4. Director, Marine Corps Research Center 2
   MCCDC, Code C40RC
   2040 Broadway Street
   Quantico, Virginia 22134-5107

5 Marine Corps Tactical System Support Activity 4
   Technical Advisory Branch
   Attn: Librarian
   Box 555171
   Camp Pendleton, CA 92055-5080

6. Marine Corps Representative 1
   Naval Postgraduate School
   Code 037, Bldg. 330, Ingersoll Hall, Room 116
   555 Dyer Road
   Monterey, CA 93943

7. Chairman, Code EC 1
   Department of Electrical and Computer Engineering
   Naval Postgraduate School
   Monterey, California 93943-5121

8. Professor Murali Tummala, Code EC/Tu 2
   Department of Electrical and Computer Engineering
   Naval Postgraduate School
   Monterey, California 93943-5121

9. Professor Robert Ives (LCDR USN), Code EC/Ir 2
   Department of Electrical and Computer Engineering
   Naval Postgraduate School
   Monterey, California 93943-5121

10. Dr. Ricard North. 1
SPAWARSYSCEN, D841
53560 Hull Street
San Diego, CA 92152-5001

11. LCDR Howard Pace Jr. 1
SPAWARSYSCEN, D841
53560 Hull Street
San Diego, CA 92152-5001

12. Mr. Marc Pearlman 1
GE CR&D
Building KW, Room C507
One Research Circle
Niskayuna, NY 12309

13. Maj. Kevin M. Shea (USMC) 1
350 Long Meadow Way
Arnold, MD 21012